Characterization of Binding of LILRA3 and LILRB2 to the Myelin-Associated Inhibitors and Major Histocompatibility Class I Molecules

by

Chris Morcos

A thesis submitted in partial fulfillment of the requirements for the degree of

Master of Science

In

Immunology

Department of Medical Microbiology and Immunology
University of Alberta

Abstract

The leukocyte immunoglobulin-like receptor family (LILR) is composed of inhibitory and activating receptors that are widely expressed on immune cells and interact with classical and non-classical MHC-I. Recently, several ligands have been identified for the LILRs including the three myelin-associated inhibitors (MAI): Nogo, MAG and OMgp. I hypothesized that the interaction between the LILRs and the MAIs modulate their interaction with MHC-I, and the interactions involve them in CNS immune-mediated diseases such as multiple sclerosis. We set out to characterize the interactions of the LILRs with the MAIs in multiple assays. LILRA3 and LILRB2 showed modest binding to OMgp in a direct ELISA and a cell-based flow cytometry assay. We attempted to block the binding to OMgp by pre-treating LILRA3 and LILRB2 with Nogo66, a 66 amino acid domain common to all Nogo isotypes. This however resulted in the enhancement of the interaction between the LILRs and OMgp. The binding between the LILRs and MHC-I was also enhanced when the LILRs were pre-incubated with Nogo66. Further experimentation is required to understand the dynamics of the interaction between the LILRs and Nogo66, and how it enhances their interaction with MHC-I and OMgp. Additionally, we shall determine the role of the membrane distal D1D2 domains of the binding to the MAIs. The interaction of the LILRs with Nogo and the widespread expression of Nogo-B suggest that Nogo could modulate LILR function, in contexts beyond the expected immune regulatory function of the LILRs.

Preface

Some of the research conducted for this thesis forms part of an internal collaboration led by myself at the University of Alberta, with the contribution of Dr. Heather Eaton. The leukocyte Ig-like receptor fusion proteins referred to in chapter 3 were designed by myself and cloned and purified with the assistance of Dr. Eaton. Table 2 in chapter 1 was adapted from a review publication I co-authored with Dr. Deborah Burshtyn titled "The Expanding Spectrum of Ligands for Leukocyte Ig-Like Receptors," Journal of Immunology, vol. 196, issue 3, 947-955. I was responsible for the literature review and contributed to manuscript composition and edits with Dr. Burshtyn.

Acknowledgements

I would first like to thank my supervisor Dr, Deborah Burshtyn. Her mentorship and leadership throughout this challenging project has allowed me to develop my skills as a scientist. She consistently allowed this project to be my own work, while steering me in the right direction refocusing me on the right questions to ask.

I would also like to acknowledge the members of my committee, Dr. Colin Anderson and Dr. Troy Baldwin for bringing their wealth of knowledge, expertise, and guidance to my project.

I would also like to thank the members of the lab, Kang Yu, Dr. Heather Eaton, Dr. Kinola Williams, Bara'ah Azaizeh, Dr. Li Fu, and Dr. Chelsea Davidson, who were involved in fun and countless discussions about science and other topics.

I would also like to thank friends and colleagues in the department of medical microbiology and immunology for the countless laughs and continuous support as well as members of the administrative staff: Tabitha Vazquez, Anne Giles, Debbie Doudiet, and Melissa Northmore for tirelessly working behind the scenes allowing us to focus on our research and development.

Lastly and importantly, a big thank you goes to friends and family for their continuous encouragement and emotional support.

Table of Contents

List of Tables

List of Figures

Chapter 1
General Introduction

1.1. The Immune System

The human body's defense mechanism is primarily governed by the immune system. The cells driving the immune response can be found residing in tissues or roaming and circulating throughout the lymphatic system. The primary functions of the immune system are comprised of recognising non-self or foreign antigens from self antigens found in cells and tissues of the body. This results in immune cells mounting a response against foreign pathogens invading tissues and downregulating the response once the pathogens are cleared. This downregulation or maintenance of balance between activation and inhibition of the immune response is crucial for homeostasis and avoiding autoimmunity. These checks and balances are in place due to many factors that modulate the immune response, chief of which are receptors found on the surface of cells of the immune system. These receptors either have activating or inhibiting roles, depending on their expression, their ligands, and their signalling capabilities through their cytoplasmic tails or adaptors. Paired-receptor families such as the Leukocyte Ig-Like Receptors comprise of activating and inhibitory receptors that play a role in balancing responses to foreign threats and maintaining homeostasis of the immune response.

1.1. The Leukocyte Ig-like Receptors

The Leukocyte Ig-Like Receptors (LILRs) is a receptor family located in the leukocyte receptor complex (LRC) on chromosome 19 [1]. The receptor complex comprises a variety of Ig superfamily receptors such as the killer-cell immunoglobulin-like receptors (KIRs), the leukocyte-associated immunoglobulin-like receptors (LAIRs), and the LILRs as characterized by Barrow and Trowsdale [2]. In

a recent review of the literature covering the LILRs we published, the receptor family was identified as being composed of two pseudogenes and eleven functional genes encoding five activating receptors, five inhibitory receptors, and a soluble protein [3]. The activating receptors and soluble protein are labeled with an A in their name (LILRA1,2,3, 4-6), while the inhibitory receptors are labeled with a B in their name (LILRB1-5). The LILRs are organized in two tightly arranged clusters, a telomeric and centromeric cluster, with the genes in each cluster transcribed in opposite directions as described by Hirayasu and Arase [1].

The first member of the LILR family, LILRB1, was cloned in 1997, by three different groups led by Marco Colonna, David Cosman, and Eric Long [4-6]. Progress in fully understanding and elucidating the role of the receptors however has been challenging. Determining the systemic and granular effects of immune receptors and their ligands has been historically done with mouse models. There are no true matching homologs of the LILRs in mice, which leads to a lack of deep understanding of the function of the LILRs. Paired Ig-like receptors (PIRs) were cloned from mouse cell lines and tissue, and initially identified as members of the Ig gene superfamily, with the activating PIR-A and inhibitory PIR-B structures' modeled by their cDNA sequence [7]. Later, eleven PIR-A receptors were identified, paired with the singular inhibitory PIR-B receptor, which was hypothesized as the potential homolog of the inhibitory LILRB human receptors. Another major difference between PIR-B and the LILRB is evident in their extracellular structure. PIR-B has six extracellular Ig domains, whereas members of the LILR family can have either four or two Ig domains. This discrepancy in the number of LILRB genes compared to the mouse PIR-B homolog,

suggest a divergence of the LILRBs in humans from the LRC of a common ancestor, and their subsequent independent amplification [8]. This is supported by the presence of the identical number of inhibitory LILRs in both humans and chimpanzees, with humans having more activating receptors than the common chimpanzee [9]. More recent evidence obtained through genome analysis of two bat species, *M. davidii* and *M. alecto* suggests that the divergence seen in the LILRs occurred in bats. In *M. davidii*, the LILRs underwent significant gene duplication events, along with other members of the LRC, while there is no evidence of expansion in *M. alecto* [10]. This variability in LILR sequences also extends to bovines, with expression analysis and sequence alignment pointing to the presence of six Ig domain containing PIR-like as well as four Ig domain containing LILR-like receptors in *Bos taurus,* in addition to multiple putative soluble proteins [11]. The patterns of expansion and contraction of LILR genes in different species point to evolutionary pressures driven by pathogens and ligands interacting with the gene family.

A certain functional redundancy could be expected from the presence of multiple inhibitory and activating LILR in humans. There is however variety in their expression pattern, with the LILRs found on the surface of and secreted by different cells of the immune system [3]. Genetically, polymorphisms in the LILRs are not common when compared to what is seen with the KIRs, which are highly polymorphic and have an expression pattern limited to NK cells and a subset of T cells [12]. Despite having limited polymorphisms, variance in the LILRs have been associated with increased susceptibility to immune-mediated diseases, such as rheumatoid arthritis, systemic lupus erythematosus, and multiple sclerosis [1]. The

more pronounced polymorphism in the gene family is seen in LILRA3 and LILRA6. A screen of a healthy Caucasian group reveals that more than 30% have two or more copies of LILRA6 [13]. On the other hand, frequent absence of a functional LILRA3 due to the deletion of most of the gene was found in several studies covering different populations [1]. The LILR locus on chromosome 19 has been fully sequenced which led to the generation of evidence pertaining to the expression of these molecules, as well as their association with immune-mediated diseases. The focus of my thesis however is on two members of the LILR family, LILRB2 and LILRA3. Significant strides have recently been made in characterizing them, but this all started with the significant work that has been done on LILRB1. While all the LILRs have been cloned and identified, not all LILRs have had their function or ligands identified.

1.2. The Leukocyte Ig-Like Receptor 1 (LILRB1)

As previously mentioned, LILRB1 was the first LILR cloned and is also the most well characterised member of the LILR family of receptors. Results generated from studying LILRB1 have led to predictions and assumptions about other members of the LILR family. This is due to the sequence but also structural similarities the LILRs have to each other as LILRB1, LILRB2, and LILRA3 share more than 80% sequence similarity when excluding the transmembrane regions and cytoplasmic tails (Figure 1 and Table 1).

Figure 1.1: Protein sequence alignment of the extracellular portion of LILRB1 (Q8NHL6.1), LILRB2 (Q8N423.4), and LILRA3 (Q8N6C8.3). Multiple sequence alignment performed on Clustal-Omega.

Table 1: Identity matrix between LILRB1, LILRB2, and LILRA3 based on the multiple sequence alignment of their protein sequence.

Proteins	LILRB1	LILRB2	LILRA3
LILRB1	100%	81.09%	83.83%
LILRB2	81.09%	100%	80.14%
LILRA3	83.83%	80.14%	100%

Percentage identity based on protein multiple sequence alignment excluding the transmembrane and cytoplasmic domains. Analysis done on Clustal-Omega.

The first ligands identified for the LILRs was the major histocompatibility complex I (MHC-I) mimic UL-18, a cytomegalovirus-(CMV) expressed protein [6]. Following the identification of the MHC-I mimic as a ligand of LILRB1, came the identification of human MHC-I as the endogenous ligand of both LILRB1 and LILRB2 [14]. In addition to identifying the first ligands, the amino acid sequence of all the LILRs was determined and their structure was predicted based on bioinformatic analyses. The discovery of the LILRs and their similarities to the KIRs led to the question as to how functionally different were these receptors from the KIRs. While they shared the MHC-I molecules as ligands, high LILRB1 expression was initially identified by flow cytometry on the surface of B cells and Monocytes. Low levels of expression of LILRB1 were seen on NK cells and T cells, the major subtypes expressing KIRs [6]. The relatively high level of expression on monocytes was confirmed when LILRB1 and LILRB2 were found expressed on both monocytes and dendritic cells isolated

from PBMCs [15]. A group led by Borges co-ligated LILRB1 or LILRB2 with the Fcγ receptor I, which led to the inhibition of phosphorylation of the tyrosine motif of the Fc receptor γ chain. The inhibition of tyrosine phosphorylation by LILRB1 or LILRB2 is mediated through SHP-1, which was recruited to the phosphorylated tyrosine tails of either LILRs [15]. Structurally, LILRB1 and LILRB2 are similar in their extracellular domains, being composed of four Ig-like domains. However, their cytoplasmic tails differ in the amount of tyrosine-based motifs. LILRB1 is composed of four tyrosine motifs compared to LILRB2's three [3]. Two of LILRB1's four tyrosine motifs are confirmed immunoreceptor tyrosine-based inhibitory motifs that are required for SHP-1 docking, and thus the receptor's ability to exert a regulatory function [16]. The inhibitory function of LILRB1 also extends to NK cells, whereby LILRB1 on the surface of NK cells inhibited NK-mediated cytotoxicity when the CMV MHC-I mimic UL18 engaged LILRB1. This was suggested as an immune-evasion mechanism employed by the human CMV virus, with UL18 being expressed on the surface of infected cells not targeted by LILRB1 expressing NK cells for killing [17]. Following the identification of UL18, an MHC-I mimic, as a LILRB1 ligands, MHC-I was also shown to engage LILRB1 which led to an inhibitory response in LILRB1-expressing cells. This inhibitory function of LILRB1 was extended to a subset of T cells that have detectable levels of the receptor's expression [18].

Questions arose regarding the characteristics of the interaction between LILRB1 and MHC-I molecules. MHC-I consist of four domains, the α1 and α2 chain are highly polymorphic and contain the peptide loading groove involved in antigen presentation.

The membrane proximal domains are the least polymorphic and consist of the α3 chain and the β2m domains. The interaction between LILRB1 and MHC-I was shown to occur between the membrane distal D1 and D2 Ig domains and the relatively less polymorphic α3 domain of MHC-I [19]. The reliance of LILRB1 on engaging the α3 domain of MHC-I confers to the receptor the ability to bind the diverse alleles of MHC-I. Functional assays however have shown that LILRB1 binds preferentially or selectively to certain MHC-I alleles [3, 20]. While studies on LILRB1's function were limited to *in vitro* work due to a lack of clear murine homolog, the more recent studies have focused on LILRB1 polymorphisms; how they associate with immune-mediated diseases and affect its interaction with its known ligands [21, 22].

More recently however, an expanding body of research has worked on the identification of new ligands for the LILR family (Table 1), and of prime interest to my own research, the identification of new ligands of LILRA3. Other pathogens were also shown exploiting the immunoregulatory function of LILRB1, with the Dengue virus, *Escherichia coli*, and *Staphylococcus aureus* engaging the receptor [3]. Dengue virus was shown to bind to LILRB1 expressed on the surface of monocytes, which in turn led to the downregulation of expression of the anti-viral IFN-stimulated genes [23]. No functional studies were done with human LILRB1 and its interactions with *E. coli* or *S. aureus*. However, a study in mice showed that the interaction between PIR-B and *S. aureus* led to the suppression of the inflammasome. The study group was also able to show that the *Pir-b* deficient mice were able to clear the *S. aureus* infection more effectively than the wild type mice [24]. While the majority of the newly identified ligands are pathogens or pathogen-derived, the endogenous calcium-

binding proteins S100A8 and S100A9 were also added to the list of LILRB1 ligands [25]. The interaction between S100A9 and LILRB1 on the surface of NK cells was shown to promote anti-HIV activity of NK cells against HIV-infected monocyte-derived dendritic cells *in vitro*. The authors however have not controlled for the potential expression of the toll-like receptor 4 (TLR 4) on the surface of NK cells, as it was suggested that the TLR4 was also a receptor for S100A9 [26]. This was the first study of its kind to demonstrate a potentially activating role for LILRB1, and further studies would need to be done to confirm the function of the receptor in the contexts of its interactions with its ligands and viral infections.

1.3. The Leukocyte Ig-Like Receptor 2 (LILRB2)

LILRB2 is similar in structure to LILRB1 in that it has four extracellular Ig domains, but three tyrosine-based motifs in its cytoplasmic tail compared to LILRB1's four. The similarities with LILRB1 continue where they share the MHC-I as ligands, with differences in binding affinities and specificities to the different class I HLA alleles. These binding modalities are evident in the crystal structures of both receptors. Both LILRB1 and LILRB2 contact the α3 chain and β2m domain of MHC-I. However, LILRB1 favours binding to the β2m domain of MHC-I while LILRB2 favours the α3 chain [27]. These binding properties by extension aligned with the fact that only LILRB2 was shown to interact with β2m-free forms of HLA-G and HLA-B27, with the latter having potential implications in autoimmunity through genetic associations and improper peptide loading [28]. In addition to the differences in contact sites, computer models of the D3D4 membrane proximal domains of LILRB1 and LILRB2

uncovered potential effects these domains have on the receptors' interactions with MHC-I molecules. The D3D4 domains of LILRB2 were suggested to clamp down onto the highly polymorphic α1α2 domains of MHC-I. This is in contrast to the lack of involvement the D3D4 domains of LILRB1 have in its interaction with MHC-I [29].

In terms of expression patterns, LILRB2's expression is limited to antigen presenting cells including monocytes and subsets of dendritic cells [3]. The first functional study LILRB2 and its function as a regulatory receptor was done in the context of transplantation. Alloantigen-specific T suppressor cells were shown to induce the upregulation of LILRB2 on the surface of monocytes and dendritic cells. This in turn was correlated with a decrease in expression of costimulatory molecules on the surface of these APCs [30]. LILRB2's function in the downregulation of the immune response however was further confirmed in studies showing the repressive cytokine IL-10 inducing the expression of LILRB2 on dendritic cells, monocytes, as well as cell lines. This upregulation of the receptor by enhancing the promoter activity of the gene in turn led to the inhibition of T cells in *in vitro* assays [31-33]. It remains unclear how the inhibitory effect were then exhibited by LILRB2-expressing APCs onto $CD4^+$ T helper cells in the reports.

The more recent development in understanding the role of the LILRs came in the discovery of novel ligands for these receptors, with LILRB2 at the forefront of the LILR family. In 2008, the first family of ligands identified for LILRB2 was the myelin associated inhibitors (MAIs) which include myelin associated glycoprotein (MAG, also known as Siglec-4a), oligodendrocyte myelin glycoprotein (OMgp), and

Nogo (also known as Reticulon 4). Atwal and colleagues expressed LILRB1, LILRB2, LILRB4, and PIR-B on the surface of COS cells and exposed the myelin associated inhibitors to the receptor-expressing COS cells to assess their binding. The authors were able to show that only LILRB2 and PIR-B exhibited binding activity to the myelin-associated inhibitors. While the group was not able to pinpoint which domains in LILRB2 or PIR-B engaged the myelin associated inhibitors, they were able to identify the 66 amino acid loop domain in Nogo termed Nogo66 as the main point of engagement from LILRB2 and PIR-B [34]. The next set of ligands identified for LILRB2 were the non-classical MHC-I molecules CD1c and CD1d [35] as well as several members of the angiopoeitin-like protein family [36]. A year later, the same group that identified the MAIs as ligands of LILRB2, found the receptor's expression was slightly upregulated in the brain tissue of Alzheimer's patients, albeit no cell-specific expression in the brain was determined, and the higher expression level was considered to be statistically non- significant likely due to the experiment being underpowered. The elevated expression levels of LILRB2 could be attributed to invading macrophages or residing microglia expressing a higher level of the receptor due to the inflammatory state. The same study also identified LILRB2 as a receptor to the Aβ42 oligomers, which are believed to be the root cause of Alzheimer's pathophysiology [37]. The Schatz group was also able to determine that the membrane distal D1D2 domains of both PIR-B and LILRB2 were required for the binding to the Aβ42 oligomers. LILRB1 and LILRB3 had no binding activity whatsoever to the oligomers. In addition to mapping the domains involved in the interaction between LILRB2 and Aβ42, the signalling pathway in the context of the

PIR-B-Aβ42 was also determined. Cofilin was recruited in the pathway, with SHP-2 also playing a role potentially upstream of it when PIR-B was engaged by the Aβ42 oligomers. Finally, the most recently identified ligand for LILRB2 was complement fragment C4d, with the second variant of LILRB3 also identified as a receptor for C4d [38]. This was the first description of receptors for C4d. In addition to C4d, a host of other complement fragments also known as complement split products (CSPs) were identified as ligands for LILRB2 including C4b, C3d, C3b, and iC3b. CSPs are a result of regulating the complement response and enzymatic cleavage of C4b and C3b. The group was able to show that LILRB2 behaved as a scavenger receptor on the surface of monocytes, by binding to soluble C4d and internalizing itself thereby resulting in cellular uptake of the C4d fragment. The signalling pathway for this endocytic-like function has yet to be determined, as Hofer and colleagues did not pursue identifying the signalling modalities involved following C4d engagement [38].

With the explosion of new ligands identified for LILRB2, a major challenge arises to identify the ligand-specific functions of the receptor. While some groups have attempted to uncover the functions of LILRB2 when interacting with some of these new ligands using *in vitro* reductionist approaches, they remain short of revealing LILRB2's systemic function in these contexts. Others however have opted to consider and thus study PIR-B as the murine homolog of LILRB2, despite the differences in structure and expression pattern. When it comes to its interaction with MHC-I, the first two membrane distal domains of PIR-B interact with MHC-I in a similar fashion to LILRB2. Differences however arise in the context of other interactions such as with the Nogo66 domain of the Nogo proteins. The six Ig

domains of PIR-B are involved in the interaction with Nogo66 as shown by surface plasmon resonance [39], with the four membrane proximal Ig domains (D3D4D5D6) having a 10-fold higher affinity to Nogo66 than the D1D2 domains. Keeping in mind these differences, studying PIR-B's function in the context of its interaction with different ligands could generate insights into the outcome of these similar interactions with LILRB2.

The first study to indirectly suggest a non-immunological function for LILRB2 was the one performed by Atwal *et al.* [34], where the myelin associated inhibitors were identified as ligands of LILRB2 and PIR-B. In addition to identifying novel endogenous non-MHC-I ligands, the authors were able to determine the function of PIR-B when it interacts with the myelin associated inhibitors. The group was also able to identify the expression of PIR-B on the surface of neurons and interacting with the MAIs on the surface of the myelin sheath surrounding the axon. This interaction led to the inhibition of neurite outgrowth, with PIR-B deficient neurons seeing an increase in growth compared to wild type neurons. The potential for LILRB2 to be involved in neuron growth and the known association of other members of the LILR family with immune-mediated diseases suggest a potential role for the receptor in similar diseases targeting the nervous system, such as multiple sclerosis. While several members of the LILR family of receptors were associated with an increased susceptibility to immune-mediated diseases and cancers, only LILRA3 was associated with multiple sclerosis [40-43].

Table 2: The Leukocyte Ig-Like Receptor family, their cellular expression, and known ligands.

Receptor	No. of Ig Domains	Expression	Ligands
LILRB1	4	Mo, Mac DC HSC B NK-subset T-subset	HLA-A, -B, -C, -F, and -G HLA-B27 H-chain dimer? CMV UL18 S100A9 *S. aureus* and *E. coli* Dengue virus
LILRB2	4	Mo, Mac DC HSC *Neuron?*	HLA-A, -B, -C, -F, and -G HLA-B27 H-chain dimer? CD1d and CD1c HLA-B27 H-chain dimer MAG, Nogo66, OMgp Angiopoietin-like protein 2 and 5 Aβ42
LILRB3	4	Mo, DC, Gran	*S. aureus* Angiopoietin-like protein 2 and 5
LILRB4	2	Mo, Mac, DC, plasmablast	?
LILRB5	4	Mo, Mac	HLA-B7 HLA-B27 H-chain dimer Angiopoietin-like protein 2 and 5
LILRA1	4 or 2	Mo, Mac DC	HLA-B27 HLA-B27 H-chain dimer HLA-C free H-chain
LILRA2	4	Mo, Mac, DC, Gran, T, NK	?
LILRA3	4	Mo, Mac, DC, B, T-Subset	HLA-C>HLA-A, HLA-G
LILRA4	4	pDC	BSA2
LILRA5	2	MO, PMN	?
LILRA6	4	Mo	?

DC, dendritic cell; Gran, granulocyte; HSC, hematopoietic stem cell; Mac, macrophage; Mo, monocyte; pDC, plasmacytoid dendritic cell; PMN, polymorphonuclear neutrophil.

The different expression patterns of members of the Leukocyte Ig-like Receptors and their respective ligands, including the number of Ig domains comprising their extracellular structure. Several members of the family don't have any ligands identified for them yet. Adapted from Burshtyn and Morcos, 2016 [3].

1.4. The Leukocyte Ig-Like Receptor 3 (LILRA3)

While LILRA3 is a member of the Leukocyte Ig-Like receptor family, it is a soluble receptor and lacks a transmembrane domain [3]. It does share similarities however in structure and sequence as previously discussed with LILRB1 and LILRB2, with four extracellular Ig domains. LILRA3's nature as a secreted protein has posed a challenge to understanding which cells expressed it. The initial studies of LILRA3 were mostly done in clinical interest due to the genetic association of the LILRA3 deletion with an increase susceptibility to multiple sclerosis. The association with MS was shown in several Caucasian populations with different groups describing the identical 6.7 kbp deletion in the gene as a risk factor [40-43]. However, these studies taken separately had small sample sizes and with the rarity of the LILRA3 deletion, the association of the deletion with an increased incidence of multiple sclerosis was weak from a statistical standpoint. On the other hand, studies in predominantly Asian populations have found a very high frequency ranging between 56% to 84% of the LILRA3 deletion manifesting itself in a premature stop codon found in exon 3 [44, 45]. The high frequency of the deletion however was not associated with any immune-mediated diseases in these populations, suggesting that the deletion on its own was not a high impact contributor to multiple sclerosis incidence, such as several HLA alleles. A more recent meta-analysis performed by Ortiz *et al.* following up on the suggestion of an association between the LILRA3 deletion and multiple sclerosis in a Spanish population [42] has instead shown that the 6.7 kbp deletion of LILRA3 had no statistically significant association with multiple sclerosis incidence [46].

The focus on these genetic associations between LILRA3 and an immune-mediated disease led to efforts to elucidate the function of LILRA3. LILRA3 being a soluble receptor was predicted to have an inflammatory function as it could potentially be an antagonist to the closely related inhibitory LILRB receptors. A study in rheumatoid arthritis patients showed constitutive LILRA3 gene expression in peripheral blood mononuclear cells (PBMCs), specifically in monocytes, B cells, and T cells [47]. However, LILRA3 protein expression was only determined in monocytes, CD4, and CD8 T cells by flow cytometry [47]. While the nomenclature of the LILR family indicates whether a member of the family is activating or inhibitory as denoted by the A or B in their name, an unexpected and sustained increased induction over time of LILRA3 expression by IL-10 in monocytes did not correspond with LILRA3's supposed activating function. The group was also able to show a slight downregulation of LILRA3 expression by monocytes when incubated with TNF-α, an inflammatory cytokine. The unexpected finding concerning the regulation of LILRA3 expression suggests a potential anti-inflammatory role for the secreted protein, with high IL-10 serum levels that can induce LILRA3 upregulation occurring in severe inflammation as a feedback loop. Finally, Tedla's group was able to correlate the levels of gene expression based on the cytokine treatment with LILRA3 protein secretion from monocytes. IL-10 led to a significant increase in LILRA3 secretion from monocytes while TNF-α resulted in the downregulation of LILRA3 levels compared to the untreated cells. On the other hand, IFN-γ treatment of monocytes led to no change over time of LILRA3 gene expression, but led to a significant increase in LILRA3 protein secretion from monocytes. The increase in LILRA3 secretion was

dependent on IFN-γ dose but also dependent on the duration of the treatment [47]. The investigators were able to identify the cells involved in LILRA3 expression, the dynamics of protein expression, and the potential immunological function of the protein, but we should cautiously interpret the study as it was done with clinical samples from rheumatoid arthritis patients, with high basal levels of inflammation.

The chase for LILRA3 ligands started with testing HLA class I molecules. LILRA3 was shown to bind to a wide array of MHC-I molecules [48, 49]. Different methods were used to identify which HLA class I molecules were LILRA3 ligands. The first study to look at HLA class I interactions with LILRA3 used LILRA3 protein purified from bacteria and surface plasmon resonance to determine LILRA3 binding affinities and domain map the interactions [48]. Comparing it to LILRB2's interactions with MHC-I molecules, the group was able to show that LILRA3 could bind to HLA-A and the non-classical HLA class I molecule HLA-G with a lower affinity. LILRB2 had a dissociation constant of 9.74 μM when binding to HLA-A*0201 and 5.62 μM when binding to HLA-G1. This mirrors the binding affinities seen with LILRB1, which also preferentially binds to the non-classical HLA-G [27]. The authors tried to explain the differences seen in binding affinity of LILRA3 to the HLA class I molecules by crystalizing the D1 membrane distal Ig domain. While similarities in sequence and thus structure with LILRB1 and LILRB2 provide LILRA3 with the capability to bind to HLA-A and HLA-G, the reduced affinity to both MHC-I molecules was suggested to be due to two amino acid changes at positions 36 and 76 [27]. The amino acid differences between the D1 domains of LILRB1, LILRB2, and LILRA3 could explain the divergence in binding affinity, but

it should be noted that the D1D2 domain of LILRA3 have a stronger binding affinity than the D1 domain only. And in similar fashion to LILRB1 and LILRB2, the D2 domain of LILRA3 is involved in the interaction with HLA class I molecules. This limits the possible interpretations about the dynamics of the interaction between LILRA3 and HLA class I molecules based on the D1 crystal structure of LILRA3. Another limitation of this study is the aforementioned bacterial purification of LILRA3. Understandably, Ryu and colleagues' objectives were to crystalize the protein, but more recent evidence suggests a biologically significant impact of mammalian post-translational modifications on LILR binding to their ligands [50]. Tagged LILRA3 was cloned and purified from *E.coli,* the *P.pastoris* yeast, or HEK293T mammalian cells. The three different purification vectors led to different glycosylation patterns. This was observed by enzymatically deglycosylating the proteins purified from the three different organisms and comparing their migration patterns on a gel. Both the in yeast and human purified LILRA3 ran further down the gel when deglycosylated, whereas the *E.coli* purified LILRA3 didn't. This was to be expected as yeast and mammalian cells can add N-linked carbohydrates to proteins whereas bacterial cells can't. The results of the deglycosylation assay suggested the presence of several N-linked glycosylation sites in LILRA3. In addition, the authors determined that natively secreted LILRA3 from donor macrophages ran identically on a silver stained gel only to the HEK293T purified LILRA3. The authors were able to identify and determine the presence of the five predicted N-glycosylation sites in LILRA3 by mass spectrometry. Furthermore, they carried on with binding and functional studies, showing that mammalian purified LILRA3 preferentially bound

monocytes in a primary culture of leukocytes and suppressed TNF-α production in PBMCs stimulated with LPS [50]. These results, in addition to the finding that LILRA3 preferentially binds to the U937 monocytic cell line over THP-1, suggest the expression of a LILRA3 specific and potentially non-HLA class I ligand on the surface of monocytes. More importantly, the group established the physiological relevance of using mammalian purified LILRA3, which was the only purified protein able to mimic the natural structure and function of native LILRA3. This finding was later supported in a study exploring the impact of glycosylation of LILRB1 and its interaction with MHC-I molecules [51]. The presence of N-linked glycans on proteins and the impact this has on function and binding will be of importance moving forward when attempting to determine the ligands and physiologic function of LILRA3.

In a comprehensive study using LILRA3 proteins purified from mammalian cells, Jones *et al* attempt to determine which HLA class I molecules LILRA3 bind to and how this binding compares to other member of the LILRs, notably LILRB2 (Figure 2) [49]. The authors used mammalian purified LILRs at a concentration of 1 μM and screened them against HLA class I single antigen beads, which consist of HLA-I molecules bound to beads. By looking at their comparative binding to the single antigen beads, LILRA3 was shown to bind to HLA-C preferentially compared to LILRB2. The group also explored the strength of the interactions between the LILRs and HLA class I free heavy chains lacking the β2m domain. The HLA class I molecules were acid treated to yield the free heavy chains conformers which consist of only the α1, α2, and α3 chains with or without a peptide, and the binding of the

LILRs to them was directly compared to their binding to native HLA class I molecules. LILRA1, LILRA3, and LILRB2 were shown to bind to the free heavy chain conformer of HLA class I molecules, whereas LILRB1 had very little binding to the β2m-free form of HLA class I. Unsurprisingly, LILRB2 was previously shown to bind to the HLA-B27 as well as the HLA-G free heavy chains, while LILRB1 was only able to bind to the β2m-associated HLA-G [27, 52]. In the case of both LILRB1 and LILRB2 where we have co-crystal structures of their interaction with MHC-I, it was previously determined that the receptors contacted the HLA class I ligands at the α3 and β2m domains. However, LILRB1 favoured the β2m domain with a dominant contact site, while LILRB2 favoured the α3 domain [27]. These differences in the favoured contact site is what likely leads to the differences seen between LILRB1 and LILRB2 and their ability to interact with the free heavy chain HLA class I molecules or not. We can therefore suggest that LILRA3's ability to bind preferentially to β2m-free HLA class I molecules could be due to the receptor favouring binding to the α3 domain of MHC-I, in a similar fashion to LILRB2. The physiological presence of HLA class I free heavy chains was shown in the following contexts: immune-mediated diseases such as spondyloarthritis, where free heavy chains of HLA-B27 were associated with the pathophysiology of these diseases, and free heavy chains expression increase on the surface of activated T cells [53, 54]. After establishing that LILRA3 could interact with several HLA-class I molecules and favoured the free heavy chain conformation, no further studies were performed on the functions of these interactions.

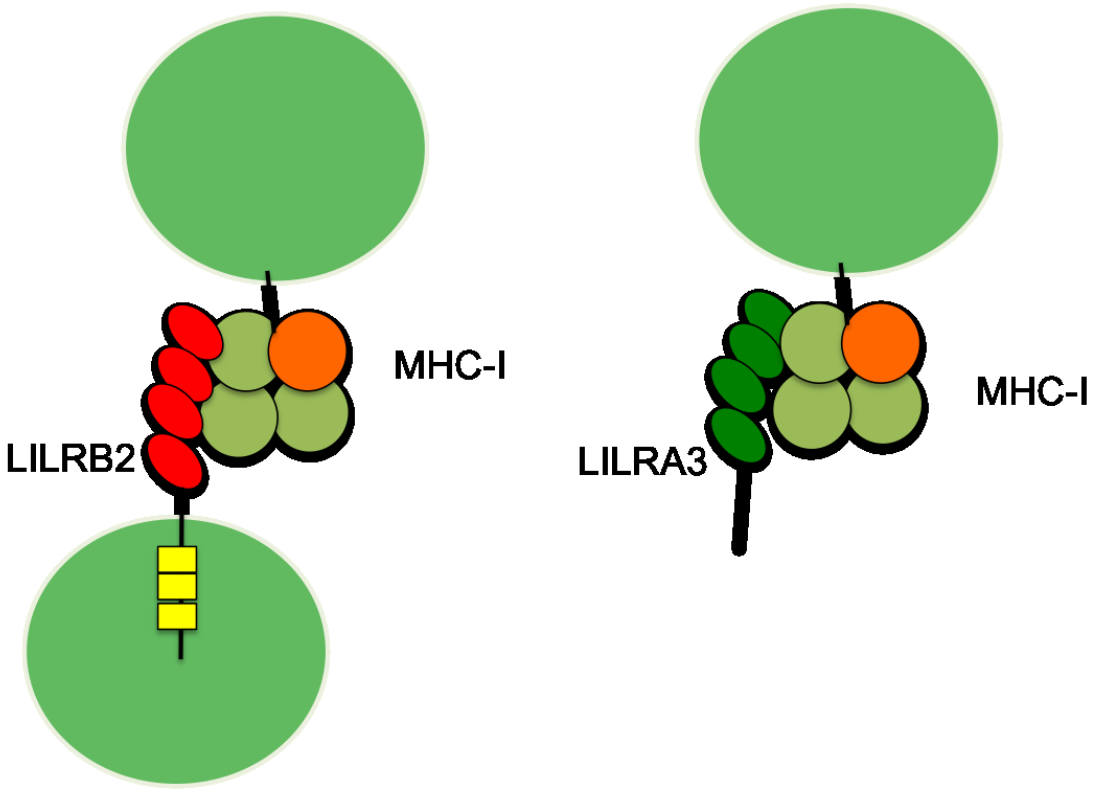

Figure 1.2: Schematic of LILRB2 (red) and LILRA3 (dark green) binding to an MHC-I (α1, α2, and α3 chains in light green and β2m domain in orange) molecule expressed on the surface of a cell. Intracellular tyrosine motifs are illustrated in yellow.

As I was conducting research for my thesis, a study came out identifying a novel ligand for LILRA3. The study was based off of the result showing that LILRA3 had a potentially non-MHC-I ligand on the surface of monocytes [50]. The group screened digested peptides for binding to LILRA3 and identified the peptides by liquid chromatography-mass spectrometry. The results returned two potential ligands for LILRA3: the Nogo66 domain common to all the Nogo isoforms and the 67 kDa laminin receptor [55]. Using surface plasmon resonance, the Nogo66 domain was confirmed as a ligand for LILRA3, with the interaction having a very high affinity. The dissociation constant for the interaction between LILRA3 and Nogo66 was in the low picomolar range, making this the strongest interaction between a LILR and its ligand known so far. The strength of this interaction suggests a physiologic function driven by the binding of LILRA3 to Nogo66. In a more biologically relevant assay than SPR, the authors assessed the binding of LILRA3 to Nogo expressed on the surface of mouse cortical neurons. The binding affinity was still high but the dissociation constant increased suggesting a decrease in affinity, with the dissociation constant being in the low micromolar range. The binding was confirmed when LILRA3 binding was lost after knocking down the expression of Nogo in the cortical neurons. Using mouse and human cortical neurons, An *et al.* were able to carry out functional assays of LILRA3 in the context of its interaction with Nogo on their surface. Incubation of neurons with Nogo66 peptide significantly decreased neurite length. However, when the neurons were co-incubated with the Nogo66 and LILRA3, a reversal was seen with neurite length significantly increasing. This suggested that LILRA3 inhibited the inhibition of neurite outgrowth mediated by the

Nogo66 peptide [55]. These findings, combined with the findings of Atwal *et al* [34], suggest that LILRA3 could potentially act as an antagonist to LILRB2 when interacting with the Nogo66 domain of Nogo. What has yet to be elucidated is whether LILRB2 is indeed expressed on human neurons, as PIR-B was shown to be expressed on mouse neurons [56]. Furthermore, we understand that LILRB2 not only interacts with the Nogo66 domain of Nogo, but also interacts with OMgp and MAG, the other members of the myelin associated inhibitors. Whether LILRA3 also behaves as an antagonist to LILRB2's interactions with both of these molecules is yet to be determined.

Before exploring the potential for these interactions, it is crucial to understand the role of the myelin-associated inhibitors, their expression patterns, known receptors, and whether they contribute to known pathologies.

1.5. The Myelin-Associated Inhibitors (MAIs)

The identification of the myelin-associated inhibitors began with the determination that myelin, in addition to it's primary neuron insulating function, had the ability to inhibit neuron regeneration following injury [57]. The discovery of the specific myelin molecules involved in the inhibition of neuron regeneration started in the 1980s when an antibody was raised against a myelin fraction responsible for the inhibition. The monoclonal antibody then named IN-1, was able to reverse the inhibition of neuron regeneration both *in vivo* and in culture. It was only in 2000 where Nogo was then named and identified as the antigen targeted by the IN-1 antibody. Subsequently, three isoforms of Nogo were identified, Nogo-A, Nogo-B, and Nogo-C. Nogo-A was the isoform identified in oligodendrocytes and the

innermost loop of myelin, where it comes in contact with the axon. The isoforms differ in size due to alternative splicing, sharing their N- and C-terminus [58]. More importantly, all three isoforms commonly share the 66-amino acid long loop termed Nogo66. LILRB2, LILRA3, and PIR-B all bind to the Nogo66 domain present on all Nogo isoforms. Nogo also belongs to a gene family called the reticulons, which are characterised by almost ubiquitous expression in eukaryotic cells [59]. Another property of the reticulons that Nogo shares is the presence of two transmembrane domains. The presence of these two transmembrane domains is hypothesized to lead to Nogo having multiple potential topologies in the cell membrane (Figure 2) [59, 60]. Highly relevant to my research presented in this thesis, the Nogo66 domain is predicted to be extracellular in both experimentally confirmed conformations. The potential of Nogo being expressed in other tissues and cells than myelin, suggest that the protein could hold different functions that may be cell and tissue-specific.

The second member of the family, the myelin-associated glycoprotein (MAG), was in fact the first member of the family to be identified as an inhibitor of neurite outgrowth, before the discovery of the IN-1 antigen. Its function as an inhibitor of neuron growth however is only limited to mature neurons, as MAG promoted the growth of young neuron [57]. Structurally, MAG is a member of the Ig superfamily, with its extracellular domains composed of five Ig domains and the four distal Ig domains are homologous to members of the sialic acid binding, Ig-like lectins (SIGLEC) family. MAG is expressed in different compartments of myelin, but to exert its inhibitory function on neuron regeneration, it is expressed in the periaxonal membrane, allowing it to be in contact with the axon.

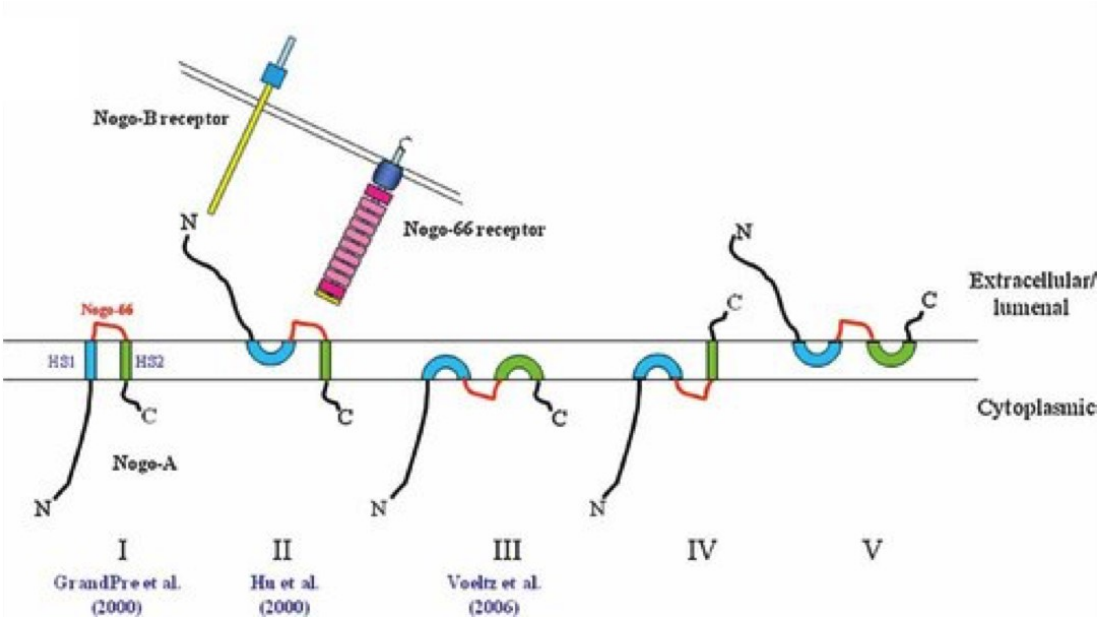

Figure 1.3: Schematic of proposed topologies of Nogo-A by different groups. Adapted from Teng and Tang, 2008. The Nogo66 loop highlighted in orange is the contact site of the interaction of LILRB2 and LILRA3 with Nogo. There is evidence to suggest that Nogo-A can exist in topologies I to IV, but there is currently no evidence to support the existence of topology V. Model II is the most likely based on data examining the interactions of Nogo-A with its various receptors.

Finally, the third and least studied member of the MAI family is the oligodendrocyte myelin glycoprotein (OMgp). OMgp does not share any structural similarities with the other two members of the family, it is a glycosyl phosphatidylinositol-linked protein (GPI), with the membrane distal domain having a cysteine-rich region, followed by leucine-rich repeats, and a serine-threonine rich domain [61]. OMgp as its name suggests is expressed by oligodendrocytes, and low levels of expression are found on the myelin sheath, mostly localized at the nodes of Ranvier [57]. The only structural similarity between the members of the MAI family are in the presence of the HNK-1 carbohydrate epitope on OMgp and MAG. The epitope is named after its presence on the surface of NK cells and is known to mediate cell-to-cell interactions [61]. The expression of the HNK-1 epitope on several proteins involved in inhibiting or activating neurite outgrowth and the finding that mice with a knockout in the enzyme genes controlling the synthesis of HNK-1, had deficiency in neural functions suggest a critical role for this carbohydrate modification [61]. The three members of the MAIs to our current knowledge also share the lack of a signalling motif or domain. Thus, for MAIs to exert the inhibition of neuron regeneration or inhibiting neurite outgrowth, they require receptors on the surface of neurons for signalling. The first MAI receptor identified was for Nogo, and was thus named the Nogo Receptor (NgR). NgR expression was identified at various levels on several neurons, and its structure was determined, being a GPI-linked receptor composed of several leucine rich repeat domains. Strittmatter's group was also able to identify that the NgR bound directly to the Nogo66 domain, and was indeed required for the inhibition of neurite outgrowth [57]. The structure of NgR however, being a GPI-linked receptor

indicate that the receptor has no transmembrane and cytoplasmic domains, leaving the question as to how the inhibition of neurite outgrowth signal is transduced in neurons. The answer came indirectly when MAG was co-precipitated with the p75 co-receptor expressed on the surface of neurons, and in the absence of p75, no MAG-mediated inhibition of neurite outgrowth was observed [57]. In addition to MAG, p75 and NgR were also shown to co-precipitate with the Nogo66 domain of Nogo, and OMgp, Taking these findings together, the three members of the MAIs interact with Ngr, which creates a complex and interacts with p75 to transduce the inhibitory signal through the membrane. These interactions led to several unanswered questions, including how does the NgR receptor maintain specificity for three dissimilar ligands in sequence and structure. Furthermore, the existence of OMgp, MAG, and Nogo-A requires blocking their interaction with the NgR to see a measurable impact on axonal regeneration. The major impact on neuron regeneration was shown when a 40-amino acid sequence from the Nogo66 domain of Nogo was used to block the NgR, blocking potentially not only the Nogo-NgR interaction, but also the OMgp and MAG to NgR interactions. With all three MAIs sharing similar high affinities to the NgR [57], their expression levels on the myelin sheath and the location of axonal damage that would require growth inhibition would govern the dynamics of their interactions with the receptor.

From the three members of the MAI family, Nogo has garnered the most interest due to the known expression of some of its isoforms outside the central nervous system (CNS) and peripheral nervous system (PNS). In fact, Nogo-A is the isoform most commonly found in the nervous system, while Nogo-B and Nogo-C have varying

expression patterns outside the nervous system [59]. In addition, it was shown that the Nogo receptors NgR1, which binds to all three MAIs and NgR2, which only binds to MAG are expressed on the surface of phagocytic macrophages [62]. In addition to the Nogo receptors, we know that LILRB2 expression was identified in immune cells circulating in the periphery, which suggests contexts in which LILRB2 could interact with the Nogo-B and Nogo-C isoforms expressed outside the nervous system.

In 2009, a group explored the role of Nogo-B in tissue repair during inflammation outside of the nervous system [63]. Nogo-B expression was found in monocytes and macrophages, with Nogo-deficient monocoytes and macrophages exhibiting impaired migration, as well as decreased chemokine and cytokine secretion. A more recent report explored the intracellular expression of Nogo in monocyte-derived macrophages, showing the localization of Nogo-B in the endoplasmic reticulum and protrusions of the migratory cells [64]. The expression of Nogo-B in immune cells such as monocytes/macrophages was additionally supported by Takai's group [39]. In fact, gene expression of MAG, OMgp, and the Nogo isoforms were found at varying levels in T and B cells, dendritic cells, macrophages, and bone marrow mononuclear cells. In another report, Nogo-B expression was shown in lung airway epithelium and smooth muscle [65]. Nogo-A/B knockout mice exhibited a severe phenotypic form of allergic asthma [65], characterized by enhanced expression of inflammatory cytokines such as IL-4 and, IL-5. The model of Th2-driven lung inflammation in mice used was also marked by a severe reduction in Nogo-B expression in smooth muscle cells and airway epithelium. Another group around the same time explored the role of Nogo-B

in leukocyte transmigration and acute inflammation in a carrageenan or zymosan-induced air pouch model [66]. Mice lacking Nogo-B on their endothelial cells had a marked reduction in recruitment of either wild-type or Nogo-B deficient neutrophils to the site of inflammation. This trend carried on in a model of carrageenan-induced paw edema. Bone marrow from wild-type and Nogo-B deficient mice were engrafted into either wild-type or Nogo-B deficient hosts. Swelling and macrophage recruitment to the site of inflammation were greatly reduced only in the Nogo-B deficient hosts, regardless of the source of the engrafted bone marrow. In addition, bone marrow from Nogo-B deficient mice engrafted into wild-type mice had similar recruitment to bone marrow from wild-type mice [66]. This suggests that endothelial Nogo-B mediates the recruitment to and transmigration of leukocytes into the site of inflammation. The authors of the study followed up by assessing neutrophil and monocyte migration by knocking down Nogo-B in human dermal microvascular endothelial cells (HDMECs). Monocytes and neutrophils had a significant decrease in their ability to undergo transendothelial migration through HDMECs with a reduction in Nogo-B expression [66]. These studies suggest that Nogo-B mediates the inflammatory process of leukocyte recruitment and migration into the tissue in different models of inflammation. Nogo-B having an immune function is of interest to us in the context of its interaction with the LILRs in humans or the PIRs in mice, however a direct implication of a Nogo-B and PIR-B interaction had not been uncovered yet in the context of inflammation.

The first study to my knowledge that explored the role of Nogo-B and its interaction with PIR-B in the periphery was conducted in mouse and human vein graft models

[67]. The model consists of grafting veins into arterial circulation, leading to the physiological adaptation of veins to the new environment, a requirement for successful grafts. The authors were able to show that in both mice and humans, veins had basal levels of PIR-B or LILRB2 and Nogo-B gene expression, which increased in grafted veins. While the authors used human vein grafts, they still however measured PIR-B expression, which does not indicate which human LILR rose in expression levels. The authors should have indicated which specific human LILR were they studying, since based on the expression profile, they could have been referring to multiple LILRs. This could also suggest that the rise in PIR-B expression they observed was not specific to LILRs when experimenting in a human model. Functional assays in this study were done in the mouse model, with PIR-B knockout derived macrophages showing an increased ability to bind to endothelial cells and infiltrate the tissue. This increase in inflammatory activity was also shown with wild-type PIR-B derived macrophages and Nogo-B deficient endothelial cells [67], suggesting a regulatory function from the outcome of the interaction between PIR-B and Nogo-B in the aforementioned model of inflammation.

To summarize, Nogo has different functions based on its expression on varying cell types and in different tissues. Nogo-A is predominantly expressed in the nervous system, while Nogo-B was shown to be expressed on endothelial cells and mediate tissue inflammation. The role of Nogo-A in inflammation of the nervous system has not been directly studied, although it has a function as a myelin-associated inhibitor which play a role in neurodegenerative pathologies. The interactions between the MAIs and the LILRs suggest their involvement in inflammatory responses and more

specifically neuro-inflammation, which inspired the work in my thesis. Conditions such as multiple sclerosis come to mind, which involve immune-mediated damage to neurons followed by neural degeneration and axonal loss.

1.6. Multiple Sclerosis

Multiple sclerosis (MS) is an immune-mediated disease of the CNS, and is characterized by variable progression states and pathophysiology [68]. The two most common seen forms of MS are relapsing-remitting MS followed by the secondary progressive state of the disease, while the other common form is the primary progressive disease. MS is characterized by an initial phase of infiltration of immune cells from the periphery into the CNS, driven by primarily by Th1 and Th17 cells and their mediators targeting self-antigens mostly derived from the myelin sheath. This leads to repeated bouts of inflammation in the CNS followed by remission in the case of relapsing-remitting MS. Ultimately, the diseases progresses into a phase characterized by axonal degeneration due to the extent of the damage caused by the inflammation. This phase is the hallmark of the secondary progressive and primary progressive forms of MS [68]. Therefore, understanding and targeting the initial inflammatory process as well as the neural degeneration phase from a therapeutic standpoint have been of interest to treat multiple sclerosis.

There are multiple mouse models used to study multiple sclerosis, with the most popular being the experimental autoimmune encephalomyelitis model (EAE). The EAE mouse model has its limitations, but a deep understanding of MS pathophysiology and the development of potential therapies rested on the study of this

model. Inducing multiple sclerosis-like disease in the EAE model is driven by the peripheral immunization with the following antigens: myelin oligodendrocyte glycoprotein (MOG), proteolipid protein (PLP), and myelin basic protein (MBP). These self-antigens were also identified in human MS patients through collected epitope data [69]. In addition, MAG and OMgp were also identified as self-antigens and targeted by the immune system in MS patients, albeit to a lesser extent than MBP, PLP, and MOG. This leaves Nogo as the remaining member of the MAIs not implicated as a targeted self-antigen based on the epitope data from MS patients.

In one report, an attempt was made to induce an EAE-like response in mice using a peptide of Nogo-A. This however did not lead to an encephalitogenic response in the mice compared to the MOG-induced model [70]. The authors however in another experiment vaccinated MOG-induced EAE mice with the Nogo peptide and observed a delayed onset of symptoms and a reduction in their severity. The same outcome was observed in MOG-induced EAE mice with Nogo-A/B/C knockout. This suggests that while Nogo may not be a suitable trigger for EAE, it plays an important role in the pathophysiology, with its absence leading to a protective effect. Supporting Nogo's function as a modulator of inflammation, the authors showed that in MOG-induced EAE mice vaccinated with Nogo, there was a significant decrease in production of inflammatory cytokines such as IFN-γ from splenocytes compared to the vaccinated control. The effect vaccinating against Nogo has on decreasing inflammation was also accompanied by a decrease in neuron degeneration [70]. This could be attributed to the production of anti-Nogo antibodies, blunting the inhibition of neurite outgrowth, allowing for the repair of damaged neurons from the inflammation.

A deeper understanding of the role of MAIs is required in the context of multiple sclerosis due to their impact on the pathophysiology. Furthermore, it would be of interest to understand whether the interaction of LILRB2 and LILRA3 with the MAIs contributes to disease progression or remission. Early studies suggested a linkage between a LILRA3 gene deletion and susceptibility to MS in different populations [42, 43]. However the absence of a LILRA3 gene in high-powered studies did not support its association with an increase susceptibility to MS, a recent report in North American MS patients has uncovered associations between serum levels of LILRA3 and the disease [71]. A two-fold increase in LILRA3 serum concentration was observed in MS patients compared to healthy controls. A further two-fold increase in LILRA3 concentration was seen when comparing patients with the severe primary progressive form of MS compared to the less severe relapsing-remitting manifestation of MS. Based on the literature covered, these results would suggest a surprising correlation between high LILRA3 expression and disease severity. The authors of this study however were only able to perform a short-term longitudinal study over 12 months, following the MS patients' clinical scores and LILRA3 serum levels. With the caution that this experiment was done on a small patient pool, patients with worsening disease after 12 months had a significant decrease in serum LILRA3 levels. On the other hand, patients who have seen an improvement in symptoms had on average higher LILRA3 serum level [71]. This correlation could be attributed to the fact that LILRA3 expression is induced by IL-10, an anti-inflammatory cytokine. Increased levels of IL-10 in the serum could be associated with inflammation resolution, which has led to that association between relatively higher LILRA3

concentration in the serum and clinical score improvement. This reinforces the potential for an anti-inflammatory and protective function of LILRA3 in MS, but further confirmation would be required with a larger sample size.

1.7. Research Focus

The first aim of my research project was to explore whether LILRA3 and LILRB1could interact with the members of the MAIs in a similar fashion to LILRB2. The objective was to determine if LILRA3 and LILRB1 bind to OMgp, before moving on to the remaining members of the MAIs.

The second aim of my research was to understand the binding preferences of the LILRs. Historically, the primary ligands of the LILRs were the class I MHC molecules. I wanted to answer the questions of how these receptors could interact with the MHC-I molecules and members of the myelin-associated inhibitors, and determine which domains of the LILRs were required for these interactions. In addition, I wanted to uncover which MAI would be the preferred binding partner of LILRB2 or LILRA3. While my research was in progress, the Nogo66 domain of Nogo was identified as a high affinity ligand of LILRA3 [55], which allowed me to use Nogo66 as the MAI of choice for these competitive binding assays. The identification of Nogo66 as a LILRA3 ligand through a screen followed by SPR and binding assays, and subsequent functional experiments in the report have confirmed LILRA3 as an antagonist to LILRB2 interacting with Nogo66. The results presented in this thesis provide evidence of a new and interesting phenomenon in that free Nogo peptide can act in trans to facilitate LILRA3 binding to MHC-I.

Chapter 2

Materials and Methods

2.1 Antibodies, proteins, and peptides

Goat anti-human OMgp, recombinant human OMgp, LILRB1-Fc, and LILRB2-Fc proteins were purchased from R&D Systems (Minneapolis, MN, USA). LILRA3-Fc protein was purchased from AcroBiosystems (Newark, DE, USA). Nogo66 (1-40) peptide was purchased from TOCRIS (Bristol, United Kingdom). Rabbit polyclonal anti-Nogo was purchased from Abcam (Cambridge, MA, USA). PE-conjugated goat-anti human Fc IgG was purchased from eBiosciences (San Diego, CA, USA). Goat anti-human Fc IgG and AP-conjugated mouse anti-goat IgM were purchased from Jackson ImmunoResearch Laboratories (West Grove, PA, USA). Lyophilised goat serum IgG was purchased from Sigma-Aldrich (Oakville, ON, Canada). W6/32 and 51.1 antibodies (IgG2A) were obtained by hybridomas by ATCC (Manassas, VA, USA) and purified by protein-G agarose beads.

2.2 Cell lines and media

721.221 MHC-I deficient cells were obtained from Dr. Eric Long (NIH) and were cultured in Iscove's modified Dulbecco's medium, 10% heat inactivated fetal bovine serum (FBS), 2 mM L-glutamine, and 1X antibiotic-antimycotic solution. 721.221-HLA-G and 721.221-OMgp cells were cultured in 721.221 media with the addition of 0.5 mg/mL G418 or 1 μg/mL puromycin respectively. K562 cells were obtained from Dr. Kevin Kane (University of Alberta) and cultured in Iscove's modified Dulbecco's medium, 10% heat inactivated FBS, 2 mM L-glutamine, and 1X antibiotic-antimycotic solution. COS-7 cells were obtained from Dr. Kevin Kane (University of Alberta) and cultured in Dulbecco's Modified Eagle's Medium (DMEM), 10% heat inactivated FBS, 2 mM L-glutamine, and 1X antibiotic-antimycotic solution. Phoenix

Cells were obtained from Dr. Silvia Vidal's laboratory (McGill) and cultured in DMEM, 10% heat-inactivated FBS, 2 mM L-glutamine, and 1X antibiotic-antimycotic solution.

2.3 Constructs

LILRA3-Fc.

Full length LILRA3 cDNA in pCMV-XL4 was purchased from Origene (Rockville, MD, USA). LILRA3 without its endogenous signal sequence was amplified with flanking NheI sites. The forward primer 5'CTACTAGCTAGCGGGGCCCCTCCCCAAGC 3' and the reverse primer 5'-CTACTAGCTAGCGCCTCACCAGCCTTGGAG-3' were used to amplify LILRA3.

LILRB2-Fc

Full length LILRB2 cDNA in pCMV-XL4 was purchased from Origene (Rockville, MD, USA). LILRB2 without the signal sequence and cytoplasmic tail but with flanking NheI sites was amplified using the following primers: forward 5'-CTACTAGCTAGCGGGGACCATCCCCAAGCCCAC-3' and reverse 5'-CTACTAGCTAGCGGAACCCCCAGGTGCCTTCCCA-3'.

D1D2-LILRA3-Fc

The two membrane distal Ig domains of LILRA3 were amplified from the LILRA3-Fc construct along with the addition of a hinge region and flanking NheI sites. The following primers were used to amplify the D1D2 domains of LILRA3: forward 5'-CTACTAGCTAGCGGGGCCCCTCCCCAAGCCCACC-3' and reverse 5'-CTACTAGCTAGCCCGTCCATTCTCCCTTCAATCTTCTTAGAAACACCTGG-3'.

D3D4-LILRA3-Fc

The two membrane proximal distal Ig domains of LILRA3 were amplified from the LILRA3-Fc construct, with the addition of a hinge region and flanking NheI sites. The following forward primer 5'-CTACTAGCTAGCGAAGCCATCACTCTCAGTGCAG-3' and reverse primer 5'-CTACTAGCTAGCCCGTCCATTCTCCCTTCAATCAGGGGGTCACTCGGGTGAGTC-3' were used.

OMgp

OMgp cDNA was purchased from Origene and amplified to include a EcoRI site at the 5' end and a NotI site at the 3' end. The primers used to amplify OMgp were 5'-GAATTCATGGAATATCAGATATTGAAAATG-3' and 5'-GCGGCCGCTCAGACAGCCAGCATGACC-3'. The insert was digested with high fidelity (HF) EcoRI and HF-NotI from New England Biolabs (Ipswich, MA, USA) for 1 hour at 37°C and sub-cloned into the digested pMX-puro backbone gifted from Dr. Lewis Lanier (University of California, San Francisco).

All inserts were digested with HF- NheI from New England Biolabs for one hour at 37°C and PCR purified using a QIAquick PCR purification kit from Qiagen (Hilden, Germany) according to the manufacturer's protocol. The CD5lneg vector was provided by Dr. Eric Long (NIH) and the CD5 leader sequence and Fc tag were subcloned into pEGFP-NML3 by Dr. Li Fu (University of Alberta). The vector backbone was digested with HF-NheI for one hour at 37°C and treated with alkaline phosphatase from (NEB) for one hour at 37°C. The product was run on a 1% agarose gel for 45 minutes at 90 volts. The backbone was excised from the gel using the

QIAquick Gel Extraction kit (Qiagen) according to the manufacturer's protocol. The PCR purified insert and gel extracted backbone were ligated using a T4 ligase (NEB) for one hour at room temperature, followed by an overnight incubation at 4°C.

2.4 ELISA

The binding of Leukocyte Ig-Like Receptors (LILRs) to OMgp was determined by performing a direct ELISA. EIA/RIA 96-well plates (Corning, NY, USA) were coated with recombinant human OMgp at 25 μg/mL in $NaHCO_3$ (pH 9.6) overnight at 4°C. The wells were blocked with PBS containing 2% fraction V bovine serum albumin (BSA), and 0.1% Tween-20 for 1 hour at room temperature. LILRB1-Fc, LILRB2-Fc, and LILRA3-Fc were added at 500 nM in triplicates for 1 hour at room temperature. Each well was washed 3 times with wash buffer (PBS and 0.1% Tween-20). Goat anti-human Fc was added at a 1:1000 dilution to each well for 1 hour at room temperature, to detect the presence of the Fc tag. The wells were washed 3 times with wash buffer. Alkaline phosphatase-conjugated mouse anti-goat was added at a 1:10000 dilution for 1 hour at room temperature, followed by 3 washes with wash buffer. Five mg of PNPP substrate (Sigma-Aldrich) was dissolved in 1X diethanolamine substrate buffer for a final concentration of 1 mg/mL, added to each well, and incubated at room temperature until a sufficient colour change was observed. The absorbance was detected at 405 nm on a Enspire Multimode Plate Reader (Perkin-Elmer, Waltham, MA, USA).

2.5 Generating and purifying Fc-tagged LILRs

To purify Fc-tagged LILRs, COS-7 cells were seeded in 150 cm^2 dishes and grown till 90% confluence. Cells were washed twice with PBS and once with serum-free

DMEM. Transfection medium containing 400 μg DNA, 5 mM HEPES, 0.5 mg/mL DEAE/Dextran, and 25 μM chloroquine in serum-free DMEM was added to the cells at 20 mL per dish. The cells were incubated in transfection medium for 2.5 hours at 37°C with 5% CO_2. The cells were then shocked with PBS containing 10% DMSO for 2 minutes at room temperature, washed with serum-free DMEM, and incubated overnight at 37°C and 5% CO_2 in complete COS-7 medium for 16-24 hours. The cells were washed with PBS twice and once with serum-free DMEM, then incubated in DMEM supplemented with 1% non-essential amino acids, 2 mM L-glutamine, and 1X antibiotic-antimycotic solution. The supernatant from the cells was collected every 3-4 days, and replenished with DMEM medium containing 1% NEAA, 2 mM glutamine, and 1X antibiotic-antimycotic solution. The collected supernatants were centrifuged at 4°C at 3780g for 20 minutes, and then were filter sterilized with a 0.2 μM filter (Millipore). The collected supernatant was run on a 1.0 cm x 10 cm Econo-column (BioRad) containing a 2 mL slurry of 50% protein A/G beads (Millipore) overnight at 4°C at a flow rate of 1 mL per minute. The column was washed with 100 mL PBS then eluted with 0.05M glycine (pH 2.0) in 10 fractions, and concentrated in PBS by centrifuging at 4°C at 3780g for 20 minutes in the Amicon 30,000 molecular weight cutoff filters (Millipore). Protein concentration was determined using a micro bicinchonic acid (BCA) assay (Pierce). Protein purity was determined by Western blot and coomassie staining.

2.6 Cell lysis and protein extraction

Five to 10 million cells were harvested and washed once with PBS. Between 0.1-1 mL of lysis buffer (1% Triton X-1000, 0.15 M NaCl, 20 mM Tris pH 8.0, 1X

iodoacetamide, and 1X Roche Complete Protease inhibitor cocktail) was added to the cells and incubate for 30 minutes at 4°C. To remove the nucleic proteins, the samples were centrifuged for 10 minutes at 10,000 g at 10°C and the supernatant was collected for western blotting or coomassie staining.

2.7 Western blot and coomassie staining

Purified proteins were denatured for 10 minutes at 100°C in 4x reducing buffer containing bromophenol blue, 50% glycerol, and 5% 2-mercaptoethanol in 1M Tris pH 6.8. The samples were run on a 8-10% separating gel for 1.5 hours at 90 volts. The proteins were transferred onto a nitrocellulose membrane in a Transblot semi-dry transfer cell (BioRad) at 15 volts for 30 minutes. The membrane was blocked for 1 hour at room temperature in a PBS and LICOR buffer at a 1:1 ratio. The membrane was probed overnight at 4°C with a goat anti-human Fc antibody at 1:1000 in blocking buffer, then rinsed twice, washed once for 10 minutes with PBS/0.1% Tween-20, followed by another wash for 5 minutes. The membrane was probed with Alexa Fluor 680 conjugated chicken anti-goat antibody at 1:10000 in blocking buffer for 1 hour at room temperature. The membrane was rinsed twice with PBS and 0.1% Tween-20, then washed one time for 10 minutes and washed again for 5 minutes. The membrane was imaged on a Li-Cor Odyssey reader (Licor).

Coomassie staining (0.1% coomassie R25, 40% methanol, and 10% glacial acetic acid) was performed by staining the polyacrylamide gel for 1 hour at room temperature. The coomassie stain was decanted and destain buffer (40% methanol and 10% acetic acid) was added to the gel and incubated overnight at room

temperature. The gel was imaged on a ImageQuant LAS 4000 (General Electrics Healthcare Life Sciences).

2.8 Retroviral transduction

Phoenix cells were seeded at 2.5 x 10^6 cells in a 60 mm^2 dish. The cells were transfected with 8-15 μg of the OMgp-pMXpuro plasmid, 100 μM $CaCl_2$, and 1X HBS (50 mM HEPES, pH = 7.05, 10 mM KCl, 12 mM Dextrose, 280 mM NaCl, 1.5 mM Na_2HPO_4), which was gently pipetted into 3 mL Phoenix cell media supplemented with 25 μM chloroquine. The cells were incubated with transfection media for 8-10 hours at 37°C with 5% CO_2. The transfection medium was aspirated and 721.221 complete medium was added to the cells, and incubated for 48 hours at 32°C with 5% CO_2. To make an infection mixture, the supernatant was collected, clarified by centrifugation, and 8 μg/mL of polybrene was added. The infection mixture was added to 500,000 721.221 cells in a 24-well plate at 1 mL per well, and centrifuged at 1500 rpm for 1.5 hours. The plate was incubated for 3 hours at 37°C with 5% CO_2. The cells were then pooled into one 15 mL falcon tube, centrifuged for 5 minutes at 1200 rpm, and resuspended in 10 mL of 721.221 complete media containing 1 μg/mL puromycin, and transferred to a T25 flask. The cells were incubated for 1 week with two media changes before expression levels were assessed using flow cytometry as outlined in the 2-step flow cytometry protocol.

2.9 Two-step flow cytometry

Cells were counted in a TC20 cell counter (BioRad) and 100,000 to 500,000 cells were collected. The cells were washed once in 3 mL FACS buffer. Primary non-conjugated antibody was added to each sample at the specified concentration by the

manufacturer and incubated for 30 minutes at 4°C. The cells were washed once in 3 mL FACS buffer. Secondary conjugated antibody was added to each sample at the specified concentration by the manufacturer and incubated for 30 minutes at 4°C. The cells were washed once in 3 mL FACS buffer and fixed with 4% paraformaldehyde for 10 minutes at room temperature. The samples were run and data was acquired on an LSR-Fortessa (BD Biosciences), and the results were analyzed with FlowJo 10 (FlowJo, LLC).

2.10 Limiting dilution

OMgp-transduced 721.221 cells were counted using a TC20 cell counter (BioRad). Serial dilutions were performed to have the cells at 3 different concentrations in 10 mL of 721.221 medium: 15 cells/mL, 5 cell/mL, and 0.5 cell/mL. A third of the wells of a 96-well flat bottom plate (Corning) received 200 µL from 15 cell/mL tube, another third received 5 cell/mL, and the final third received 0.5 cell/mL. The cells were monitored every three days, with 721-221-OMgp medium changes every week. Once cell growth was observed in the final two thirds of the plate after about 8 weeks, the content of up to 15 wells were duplicated onto another 96-well plate. The growth of these cells was monitored, and once they reached confluence, OMgp expression was assessed using 2-step flow cytometry staining. Cells having a monophasic expression of OMgp were transferred to a 24-well plate (Corning), and once confluent after 3 days, were each transferred to a T25 flask (Costar) for long-term culture.

2.11 Binding assays

Regular binding assay.

Cells were counted using a TC20 cell counter (BioRad) and resuspended at a concentration of 20 million cells/mL in FACS buffer containing 2% FBS and 1mM EDTA in PBS. The cells were added at 200,000 cells per sample. Blocking antibodies were added to the cells at 50 μg/mL, and incubated for 30 minutes at 4°C. Fc-tagged fusion proteins were then added to the cells at varying concentrations, as well as FACS buffer bringing the total volume up to 20 μL. The samples were then incubated for 1 hour at 4°C. The samples were transferred to 5 mL FACS tubes and washed one time with 3 mL FACS buffer. PE-conjugated goat anti-human Fc is added at 5 μg/mL for 30 minutes at 4°C. The samples were washed one time with 3 mL FACS buffer and fixed with 4% paraformaldehyde for 10 minutes at room temperature. The samples were run and data was acquired on an LSR-Fortessa (BD Biosciences), and the results were analyzed with FlowJo 10 (FlowJo, LLC).

Binding assay in the presence of Nogo

To block the interactions between the LILR-Fc and the ligands expressed on 721.221-OMgp and 721.221-HLA-G cells, the LILR-Fc were incubated with the Nogo66 (1-40) peptide at a 1:10 molar ratio for 1 hour at 4°C. 200,000 cells were added to the complex and incubated for 1 hour at 4°C. The remaining steps were performed as outlined in the regular binding assay protocol.

Reciprocal binding assay

To determine the effects that the Nogo66 (1-40) peptide has on the 721.221, 7221-OMgp, and 721-221-HLA-G cells, the peptide was incubated with 200,000 cells for 1 hour at 4°C. The cells were washed with FACS buffer one time. The LILR-Fc were

introduced at a specific molar concentration and the volume was brought up to 20 µL with FACS buffer. The remaining steps were performed as outlined in the regular binding assay protocol.

2.12 RT-PCR

RNA was extracted from 4 million 721.221 or K562 cells using a RNeasy kit (Qiagen) followed by the QiaShredder (Qiagen) to homogenize the sample, and back to the RNeasy kit, as per the manufacturer's protocol. RNA concentration was measured using a Nanodrop1000 (Thermo Fisher Scientific). The samples were treated with amplification grade DNaseI (Invitrogen) as per the manufacturer's protocol. The One-step RT-PCR kit (Invitrogen) was subsequently used to generate cDNA from the RNA samples as per the manufacturer's protocol. The following primers were used:

- Isoform common forward Nogo: 5'- GTTGTTGACCTCCTGTACTGG-3'
- Forward Nogo A and B: 5'-ATGGAAGACCTGGACCAGTC-3'
- Forward Nogo C: 5'-ATGGACGGTCAGAAGAAAAATT-3'
- Reverse Nogo: 5'-TCATTCAGCTTTGCGCTTCA-3'
- Actin Forward: 5'-AGGGCGTGATGGTGGGCAT-3'
- Actin Reverse: 5'-TTGTAGAAGGTGTGGTGCCA-3'

The RT-PCR products were run at 1µg per well on a 1.5% agarose gel for 40 minutes at 90 volts and were imaged on a ImageQuant LAS 4000 (General Electrics Healthcare Life Sciences).

2.13 Statistical analysis

Statistical analyses including an unpaired student t-tests with the statistical significance set at $p \leq 0.05$ were performed on binding assays and indirect ELISA using GraphPad Prism 6.

Chapter 3

LILRA3 binds to OMgp, a novel ligand belonging to the myelin-associated inhibitor family

3.1. Introduction

The reported association of LILRB1 and LILRA3 with immune-mediated diseases and particularly multiple sclerosis, LILRB1's well-characterised immuno-regulatory function and wide expression pattern, as well as the sequence and structure similarities between LILRB1, LILRB2, and LILRA3, incited us to explore whether LILRB1 and LILRA3 interacted with the myelin-associated inhibitors. No other members of the LILR family aside from LILRB2 were reported to bind to these ligands, despite the sequence and structural similarities they have, and redundancies observed in binding capabilities of different LILRs to the same MHC-I molecules [3, 49]. A sequence alignment of the extracellular Ig domains of LILRB1, LILRB2, and LILRA3 shows more than an 80% similarity (Table 1) between all three proteins. I sought to explore whether LILRB1 and LILRA3, like LILRB2, could bind to the myelin-associated inhibitors (MAI). I picked OMgp as the MAI of choice to perform the experiments due to Nogo having variable conformation. MAG is a member of the SIGLEC family, having sialic acid –binding capabilities, which would be a confounding variable if it were to bind to the LILRs.

3.2. Results

3.2.1. LILRA3 binds to OMgp in a direct ELISA

To quickly determine whether there are any potential interactions between LILRB1 and LILRA3 with the myelin-associated inhibitors, I designed a direct ELISA using commercially acquired reagents. OMgp was chosen out of the three myelin-associated inhibitors due to its predictable structure, compared to Nogo and

MAG, the former having different conformations, and the latter being a member of the SIGLEC family and its ability to form interactions with sialic acid. The wells of a 96-well EIA/RIA plate were coated with 25 μg/mL of either OMgp or BSA as a negative control. Based on previous reports of binding capabilities of LILRB2 to OMgp, we used Fc-tagged LILRB1, LILRB2, and LILRA3 at 500 nM in triplicates throughout all experiments. Throughout each independent experiments, a pattern emerged showing LILRA3 having stronger binding capabilities to OMgp than LILRB2, with LILRB1 exhibiting no binding properties at all. A downside to the ELISA was the amount of background binding that was seen in LILRB2 and LILRA3 to the BSA coated wells. Furthermore, there were significant fluctuations in raw OD 405 nm numbers from day to day for repeated experiment, but the trend of LILRA3 showing the strongest binding capability to OMgp held. The results of 8 repeated independent experiments were aggregated and plotted (Figure 3.1), with LILRA3 showing specific and non-random binding to OMgp relative to BSA.

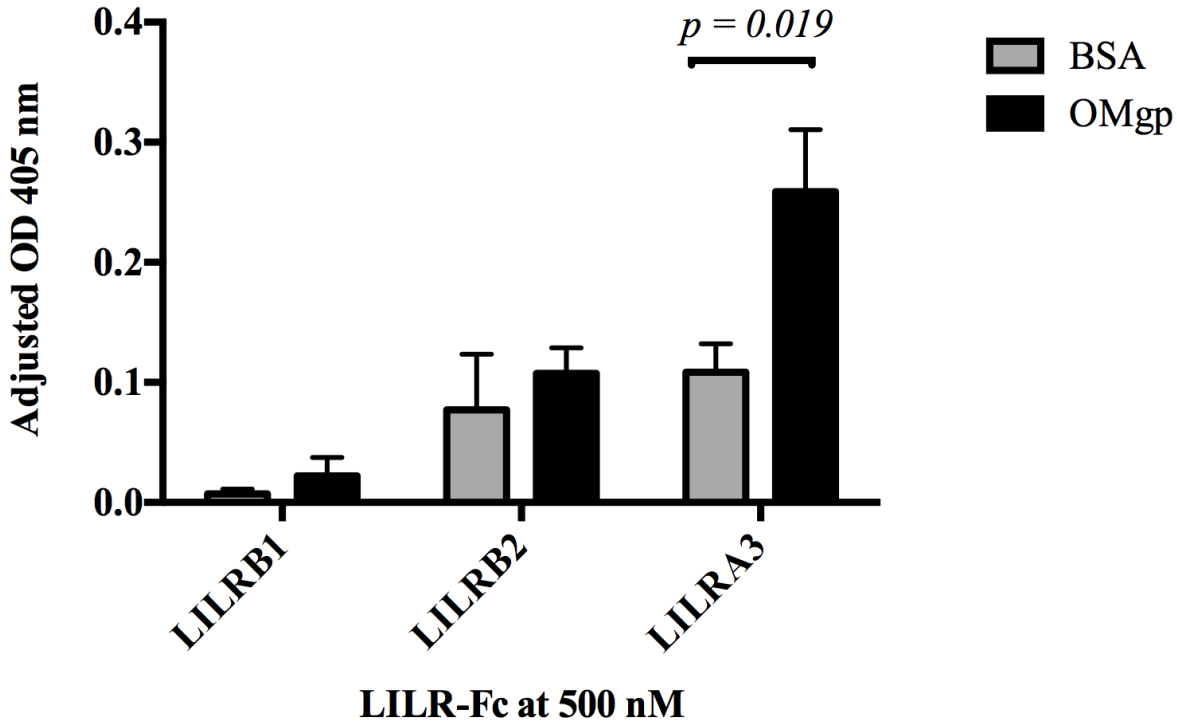

Figure 3.1. LILRA3 binds to OMgp in a direct ELISA

Wells were coated with either 25 μg/mL of OMgp or BSA. Fc-tagged LILRB1, LILRB2, and LILRA3 were added onto the wells at 500 nM. Binding of the Fc-tagged LILRs was detected by the addition of goat anti-human Fc at 1:1000, followed by AP-conjugated mouse anti-goat. PNPP substrate was added to all the wells and the absorbance was measured adjusted against the blank, at 405 nm following the colour change. Unpaired student t-test performed for the analysis, n = 8.

3.2.2. Development of 221 cells expressing OMgp

The results from the ELISA (Figure 3.1) while preliminary, suggest that OMgp is bound by LILRA3. To confirm these results, I set out to develop an assay where LILRA3 would be interacting with OMgp on the surface of a cell, thereby making the assay more physiologically relevant. The first objective was to have a MHC-I deficient cell line expressing OMgp on its surface, to minimize the background binding of the LILRs to this cell. I used 721.221 (referred to 221 cells from here on) cells, a B-lymphoblastoid human cell line, due to it's lack of surface HLA-A, B, or C expression, to express OMgp by retroviral transduction. A cDNA clone of OMgp was purchased from Origene and subcloned into the pMX-puro vector. The protocol for the retroviral transduction was adapted from Dr. Garry Nolan's group at Stanford University and optimized by Dr. Li Fu (Li Fu, University of Alberta, 2013). I transfected 15 μg of OMgp-pMX-puro DNA into Phoenix cells containing the retroviral polyprotein, envelope protein, and reverse transcriptase. I then collected the supernatant containing the packaged retrovirus 48 hours later. I infected the 221 cells with the infection mixture containing the virus and polybrene for 4.5 hours, and then incubated the cells in complete medium for 48 hours. Puromycin was added to the cells and once they reached confluence, OMgp expression was assessed by flow cytometry (Figure 3.2.A) staining of non-transduced 221 compared to 221-OMgp, which showed no expression of OMgp on the surface 221 cells. The flow cytometry histogram of 221-OMgp cells showed a biphasic expression of OMgp, an expected result from a retroviral transduction. Two discrete populations of cells were observed, one with high expression of OMgp, and the other with no detectable expression of

OMgp over the isotype control. I also assessed OMgp expression by western blot (Figure 3.2-B) after extracting protein from 10 million cells. The presence of a distinct band around 100 kDa from the 221-OMgp lysate confirmed the expression of the protein in the cells.

I attempted to use flow automated cell sorting using an anti-OMgp antibody to have a homogenous population of 221 cells expressing OMgp. I was not able to culture the cells either due to contamination, or the absence of growth of 221-OMgp cells in the flasks. I decided to clone out 221 cells with a monophasic expression pattern of OMgp by limiting dilution. Dividing a 96 well plate into thirds, I set up 32 wells with a starting concentration of 3 cells per well, 1 cell per well, or 0.1 cell per well. The wells with a concentration of 3 cells per well are expected to have a cell population grow with heterogeneous OMgp expression. The 1 cell per well and 0.1 cell per well wells would have a high probability of cell growth having monophasic OMgp expression. The cells in these latter wells would qualify as sublines of high monophasic OMgp expressors, likely clonally derived. After 8 weeks of culturing the cells, with weekly media changes, we assessed OMgp expression (Figure 3.3), and identified 5 sublines with a high monophasic expression pattern of OMgp.

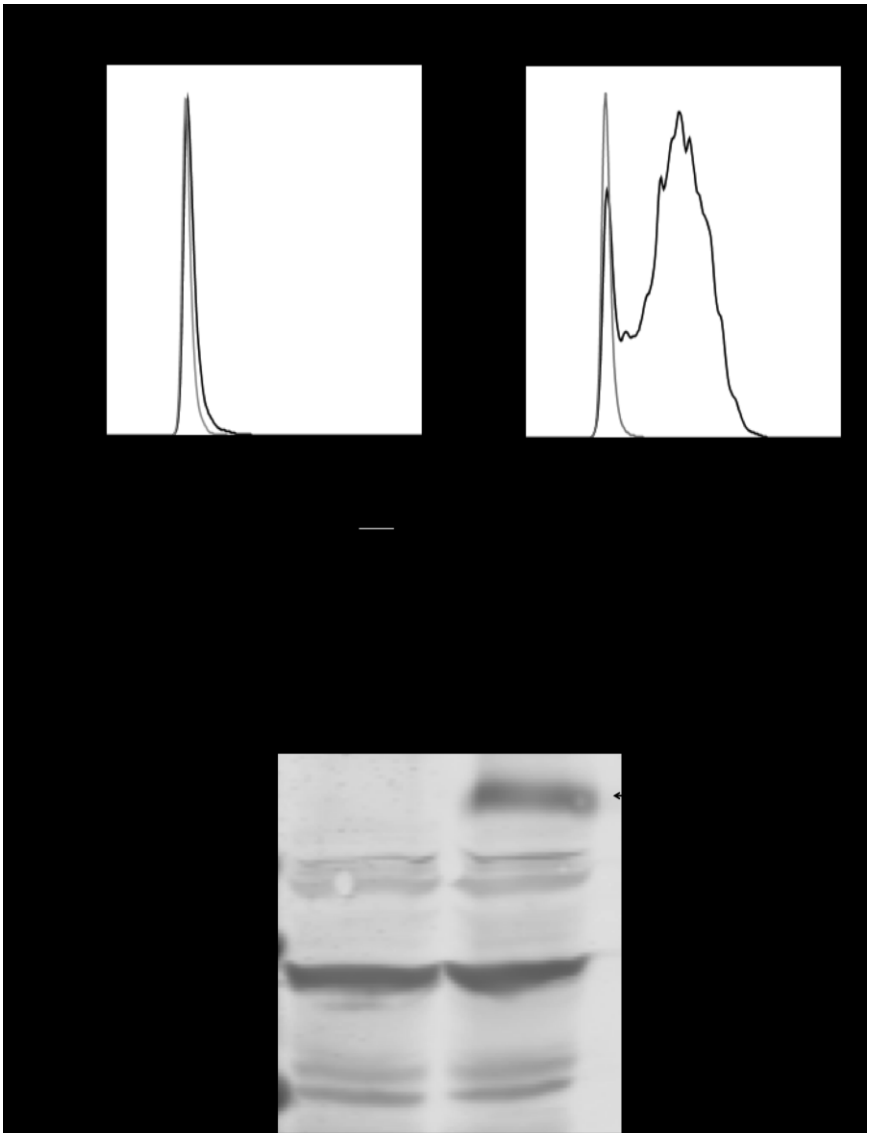

Figure 3.2. Generating OMgp-expressing 221 cells by lentiviral transduction

A) OMgp expression detected by flow cytometry of non-transduced 221 compared to OMgp-transduced 221 using goat anti-OMgp, and Alexa Fluor-647 conjugated chicken anti-goat 1 week post transduction. B) Western blot of OMgp (black arrow) from lysed non-transduced 221 compared to OMgp-transduced 221 using goat anti-OMgp and Alexa Fluor-647 conjugated chicken anti-goat 1 month post transduction. The results are representative of two repeats.

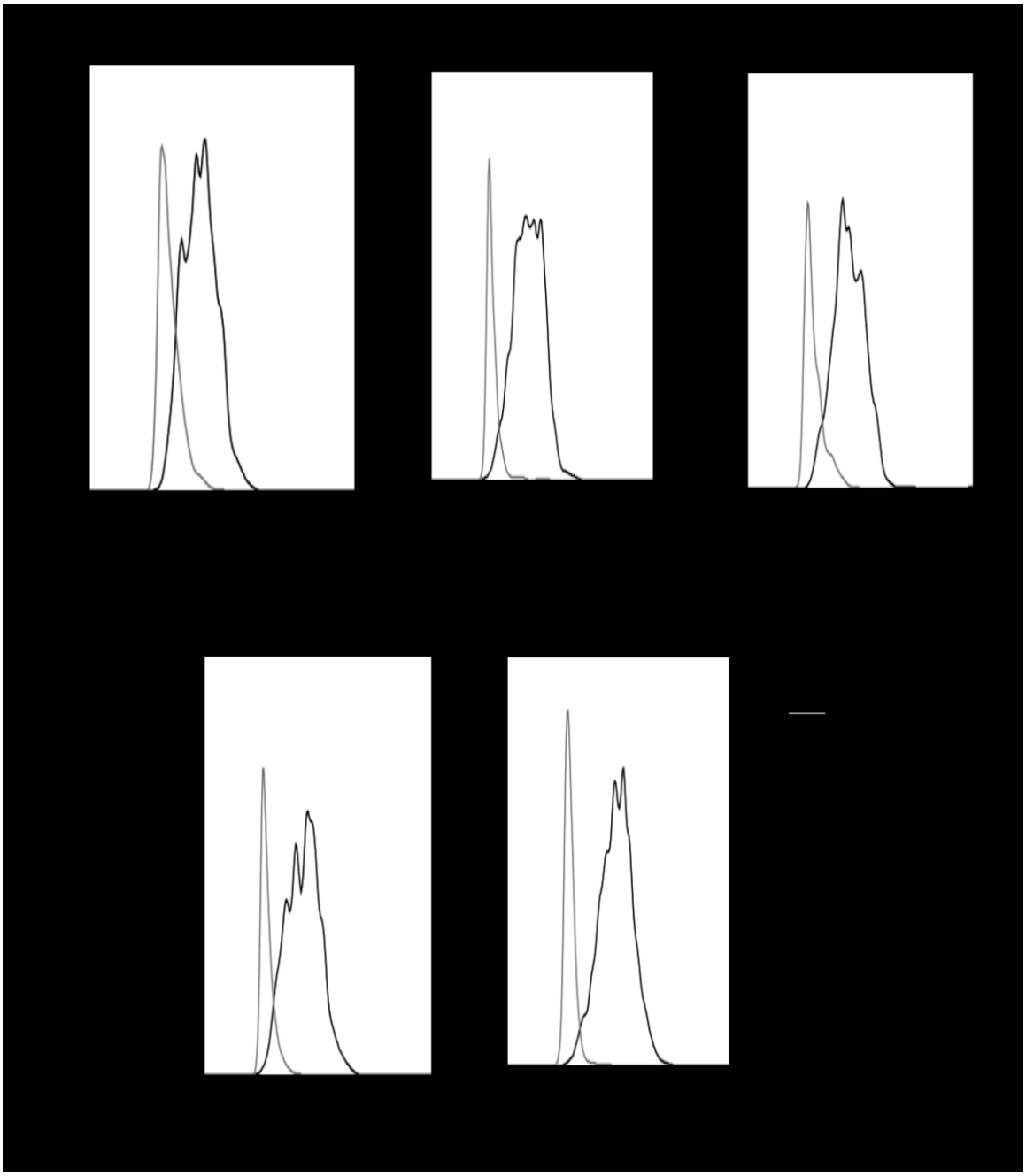

Figure 3.3. Isolation of 221-OMgp cells expressing monophasic levels of OMgp by limiting dilution.

Five OMgp-expressing 221 clones were isolated in a 96-well plate by subcloning bulk 221-OMgp cells for 8 weeks. OMgp expression was detected by goat anti-OMgp and Alexa Fluor-647 conjugated chicken anti-goat using flow cytometry.

3.2.3 Generation of soluble tagged LILRB2 and LILRA3

To assess the binding capabilities of the LILRs to OMgp, I cloned LILRB2 and LILRA3 into an Fc tag-containing vector. I also cloned with the assistance of Dr. Heather Eaton the two membrane distal domains of LILRA3 (D1D2-LILRA3), and the two proximal distal domains of LILRA3 (D3D4-LILRA3) (Figure 3.4A). To validate the production of Fc fusion proteins from our constructs, I conducted a small-scale transfection of the constructs. I also wanted to assess the relative stability and output of each construct. The constructs were each transfected at equimolar concentrations into COS-7 cells, and supernatants were collected 3, 6, and 9 days post transfection. The collected supernatants containing the purified proteins were separated by SDS-PAGE then probed for by Western blot, with an anti-Fc primary antibody probing for the Fc tag (Figure 3.4B). The transfections of the Fc-tagged LILRs were scaled up and I performed affinity tag purifications with Protein-A/G beads to capture the Fc-tagged LILRs. After the purification, I determined the concentration of the LILRs using a microBCA assay. The results from these assays, repeated each time a LILR was purified, allowed me to qualitatively and quantitatively determine the yield of the LILR-Fc based on the concentrations I obtained. D1D2-LILRA3-Fc was the protein purified with the highest yield, followed by the full length LILRA3-Fc, LILRB2-Fc, and finally D3D4-LILRA3-Fc. LILRA3 being a secreted protein, it was expected to see that the full length protein as well as the D1D2 domains had high yields as fusion proteins. However, the low yield from D3D4-LILRA3-Fc transfection suggests that the two membrane proximal domain are either unstable or aren't properly folding, affecting the secretion of the fusion protein.

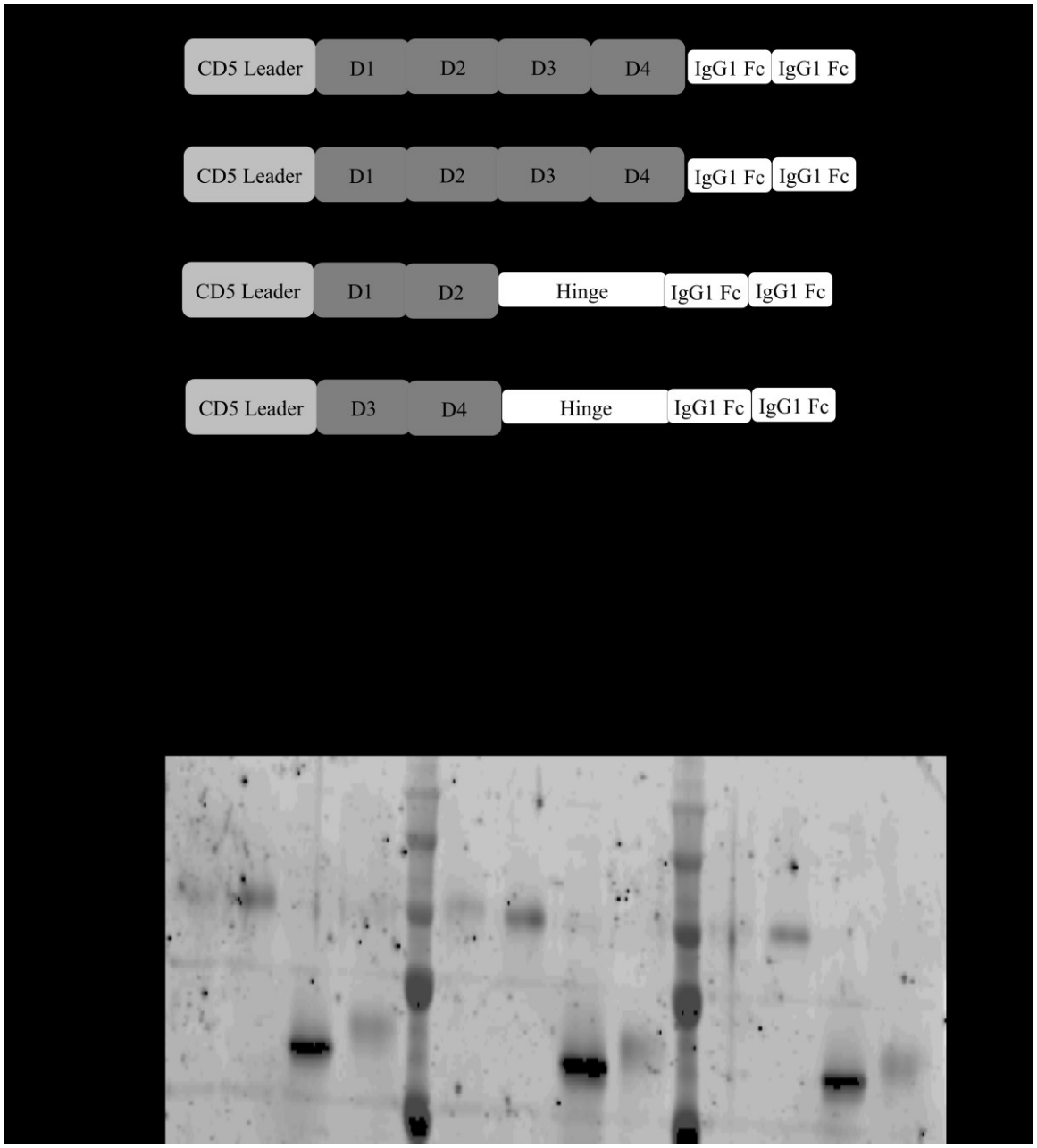

Figure 3.4. Generation of Fc-tagged LILR constructs and transfection output

A) Schematic of LILR-Fc constructs generated (not to scale). B) Western blot of collected supernatant from COS-7 cells transfected with LILRB2-Fc, LILRA3-Fc, D1D2-LILRA3-Fc, D3D4-LILRA3-Fc. LILR-Fc detected with goat anti-Fc, and Alexa Fluor 680 donkey anti-goat using a Li-Cor Odyssey. Representative blot of three experiments.

3.2.4. Purified LILR-Fc proteins bind to HLA-G

I performed binding assays with LILRA3, LILRB2, D1D2-LILRA3-Fc, and D3D4-LILRA3-Fc on 221 and HLA-G expressing 221 cells (221-G). Given that HLA-G is a known ligand of LILRA3, LILRB2, and D1D2-LILRA3, this experiment was performed to ascertain the purified proteins' functionality. I chose to use 1.5 μM of LILRA3-Fc, LILRB2-Fc, and D1D2-LILRA3-Fc for the binding assays, and was able to determine specific binding to HLA-G by adding W6/32, a known MHC-I blocking antibody. The choice of using 1.5 μM as the concentration at which to do the binding assays was due to two factors. Single antigen bead assays previously performed had used 1 μM of the LILRs to determine their binding to MHC-I molecules [49], and the different stock concentrations of the fusion proteins dictated an upper limit for the binding assays. The binding assays were performed using flow cytometry, with binding to 221 cells used as a comparator to 221-G cells, and looking at a shift in the histogram profile of the LILRs from their background binding to 221 to 221-G. I was able to block LILRB2-Fc binding to HLA-G almost completely in the presence of W6/32, compared to the isotype control. I was able to also block binding of LILRA3-Fc to HLA-G, albeit marginally (Figure 3.5.A). This could be due to the different binding dynamics LILRA3 exerts when binding to HLA-G compared to LILRB2 [48]. The binding of D1D2-LILRA3-Fc to HLA-G had a different binding profile on the histogram. In the absence of the blocking antibody, a tail was formed indicating slight binding of D1D2-LILRA3-Fc to HLA-G. The tail subsided in the presence of the blocking antibody (Figure 3.5.B). Performing binding assays with D3D4-LILRA3-Fc was a challenge due to the low stock concentration of the purified

protein, as well as the fact that there was a large amount of background seen in binding assays. This, in addition to the background binding observe with LILRA3 to 221 cells, could indicate that the D3D4 domains of LILRA3 play a role in binding to HLA-G. However, judging from the binding profile of full length LILRA3 and D1D2-LILRA3 to parental 221, it is possible that the D3D4 domains generate binding to unknown molecules on the cells. This background binding could be non-specific or driven by binding to non-HLA molecules found on the surface of 221 cells.

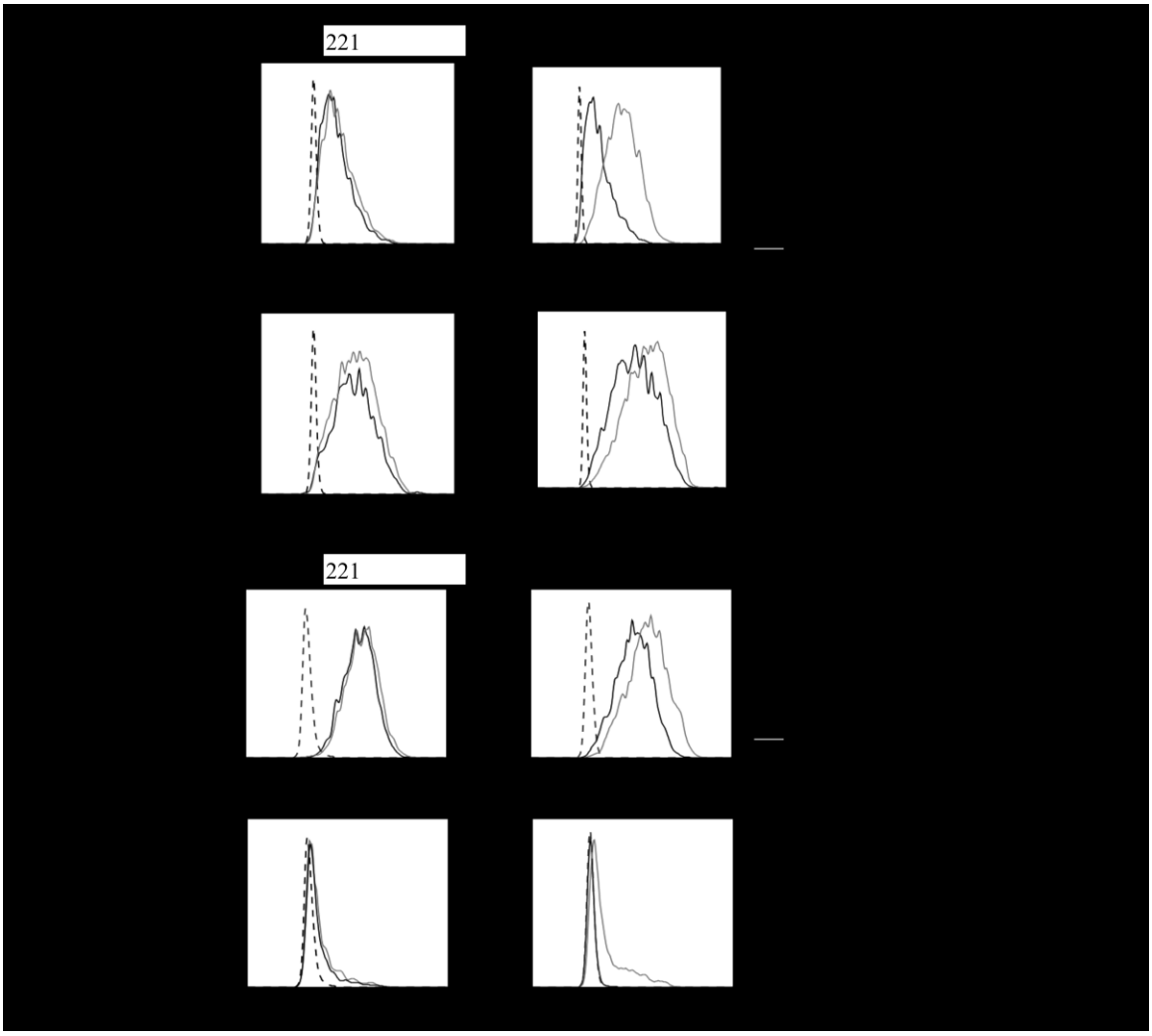

Figure 3.5. LILRB2, LILRA3, and D1D2-LILRA3 bind to HLA-G.

Representative histogram data of binding assays of A) LILRB2-Fc and LILRA3-Fc (n = 3) and B) LILRA3-Fc and D1D2-LILRA3-Fc (n = 2), binding to HLA-G on 221 cells, and blocking of the interaction by the addition of an anti-MHC-I antibody. Binding was detected using PE-conjugated anti-Fc using flow cytometry.

3.2.5. Determining the binding of LILRA3 to OMgp

Having confirmed the ability of the purified proteins to bind to a known ligand, I set out to explore whether LILRA3 could bind to OMgp. OMgp was already identified as a ligand of both LILRB2 and PIR-B, so I used LILRB2-Fc as a positive control. I chose a constant concentration at 1.1 μM of LILRB2-Fc and LILRA3-Fc binding to both 221 and 221-OMgp. The fluorescence was quantified by subtracting the geometric mean fluorescence intensity (gMFI) of the PE anti-Fc antibody binding to the cells to the gMFI of the LILR-Fc binding. Both LILRB2-Fc and LILRA3-Fc showed similar binding profiles with 221-OMgp when used at the same concentration (Figure 3.6.A). The binding of both LILRA3-Fc and LILB2-Fc to OMgp was low in terms of gMFI but reproducible (Figure 3.6.B). This could be due to the low levels of expression of OMgp on the surface of the transduced 221, or the nature of the interaction of LILRA3 and LILRB2 to OMgp being weak. To confirm that the binding of LILRA3-Fc and LILRB2-Fc to OMgp was specific, I attempted to perform similar binding assays with an anti-OMgp antibody to block the interactions. The antibody was used at different concentrations, with no effect on the binding of LILRA3 or LILRB2 to OMgp (data not shown). While the antibody was a polyclonal antibody, this suggests that the antibody did not block epitopes involved or near the contact sites of LILRB2 and LILRA3 to OMgp.

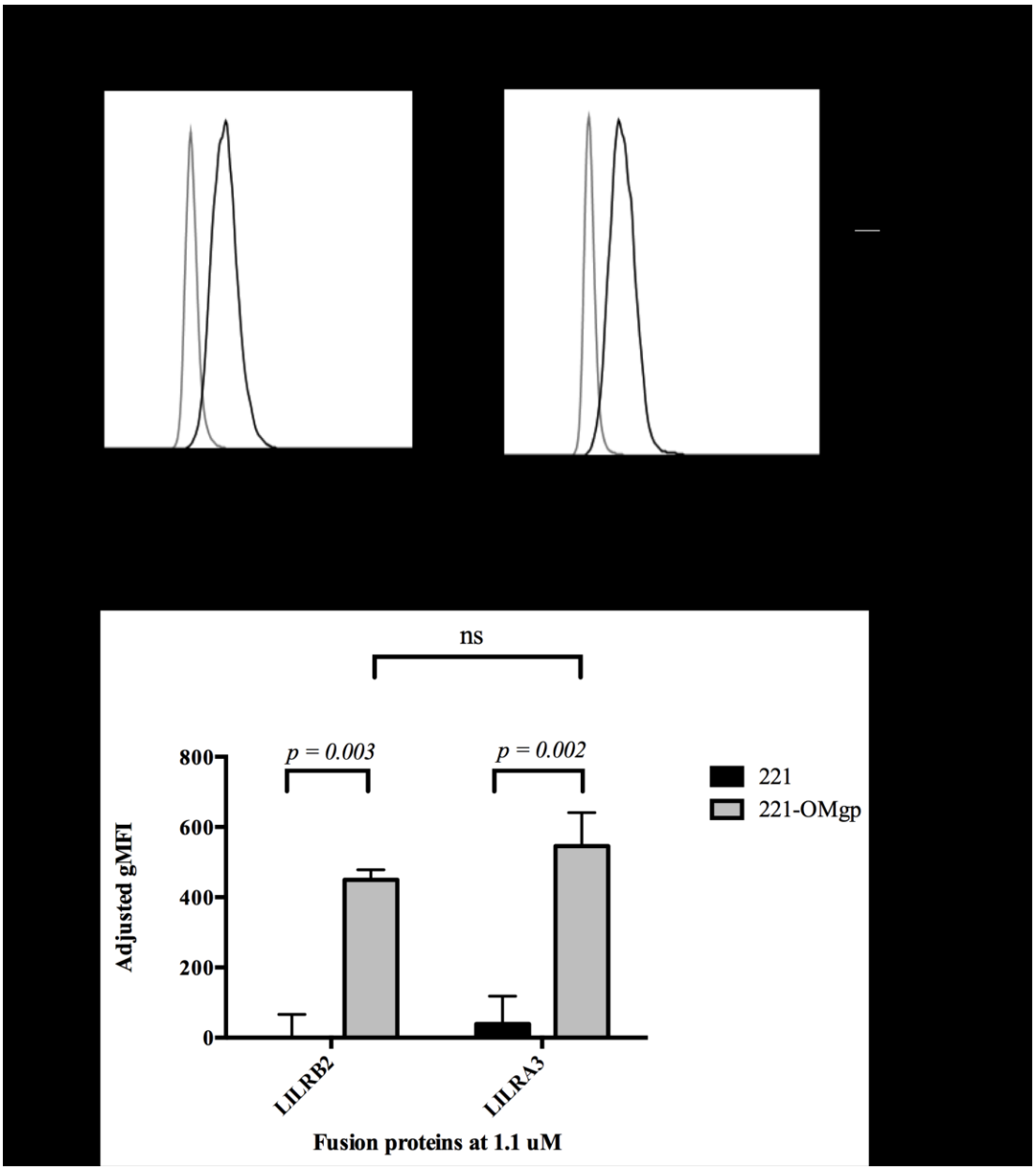

Figure 3.6. LILRA3-Fc and LILRB2-Fc bind to OMgp expressing 221 cells

A) Representative histogram of a flow cyometry binding assay of LILRB2-Fc and LILRA3-Fc binding to OMgp at 1.1 μM and B) aggregated data from two independent experiments, unpaired student t-test performed for the statistical analysis (n = 2). Binding was quantified in adjusted geometric mean fluorescence intensity (gMFI), by correcting for background by substracting secondary only gMFI to LILR gMFI.

After establishing that LILRA3 shows some binding activity to OMgp that is comparable to LILRB2, I set out to test whether the binding observed was dose dependent. The concentration of the purified LILRA3-Fc was a limitation in this experiment, as the highest concentration I could use to assess the dose-dependence of the binding experiment was 2.5 μM. The remaining concentrations at which LILRA3-Fc was used were 2, 1.5, and 1 μM. Over four independently repeated experiments, LILRA3-Fc bound to 221-OMgp cells as shown by the gMFI numbers compared to parental 221 cells (Figure 3.7). The signal relative to 221 cells was statistically significant at all four concentrations. It is however important to identify that the specificity of binding to OMgp on the surface of 221-OMgp cells can only be confirmed if the binding can be blocked.

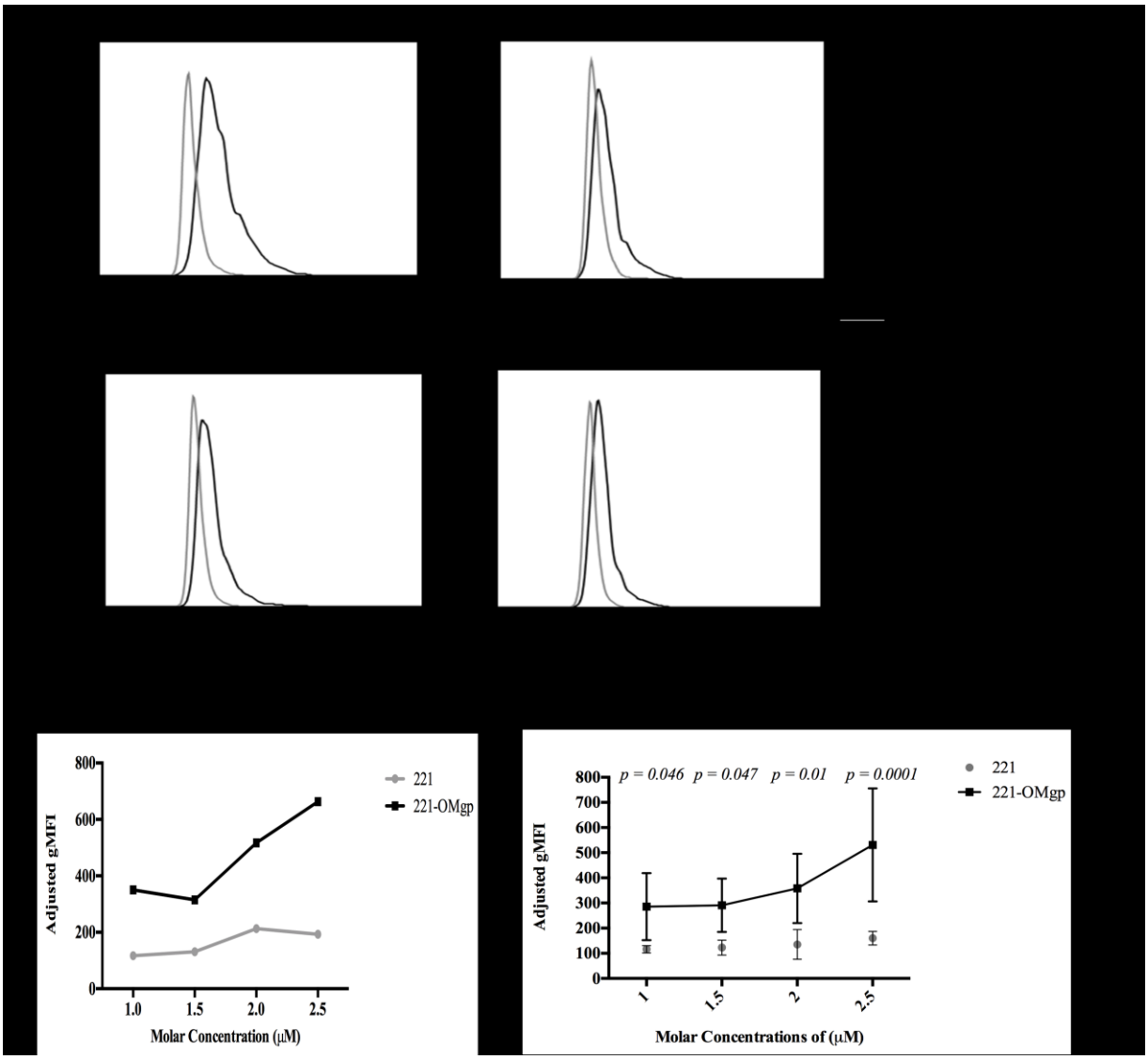

Figure 3.7. LILRA3-Fc binds to OMgp expressing 221 cells in a concentration dependent manner

A) Representative histogram data and B) plotted data of LILRA3-Fc binding to 221 OMgp cells at different concentrations. C) Aggregate data of LILRA3-Fc binding to 221-OMgp at different concentrations, unpaired student t-test performed for the statistical analysis (n = 4).

Chapter 4

Nogo66 enhances LILRA3 and LILRB2 binding in a ligand-specific manner

4.1. Introduction

While I was examining the binding of LILRA3 to OMgp, a report demonstrated that the Nogo66 domain of Nogo is a ligand of LILRA3 [55]. This study also demonstrated the role LILRA3 played as an antagonist of the LILRB2-Nogo66 interaction, thereby blocking the inhibition of neuronal outgrowth. These findings led me to ask several questions about the characteristics of the interactions between the LILRs, MAIs, and MHC-I. I wanted to determine whether the interaction between LILRA3 and OMgp would be blocked in the presence of the Nogo66 peptide. This would give us an indication of the domains of LILRA3 involved in the binding to Nogo66 and OMgp and whether LILRA3 uses a common binding site for both ligands. I also wanted to explore whether the high affinity of the interaction between LILRB2 and LILRA3 with Nogo66 would outcompete the interaction between the LILRs and MHC-I. This could shed some light on the *in vivo* role of LILRB2 and LILRA3 and the binding partners they prefer to interact with.

4.2 Results

4.2.1. LILRA3 binds to an unknown ligand on K562

As I was setting up the flow cytometry-based binding assays to explore the binding of the LILRs to OMgp, I tested the human erythroleukemia cell line K562 as a negative control for LILRA3 binding. K562 cells are commonly used cells to measure NK cell activity due to their lack of MHC-I expression [72]. I performed a couple of binding assays with LILRA3-Fc and K562 cells, with LILRA3-Fc consistently and unexpectedly binding to K562 (Figure 4.1). This suggested either the

presence of a non-MHC-I LILRA3-specific ligand expressed on the surface of K562 cells or non-specific binding due to the Fc tag. The binding of LILRA3 to K562 cells suggest a non-uniform expression of that ligand, as observed by that bi-phasic histogram profile.

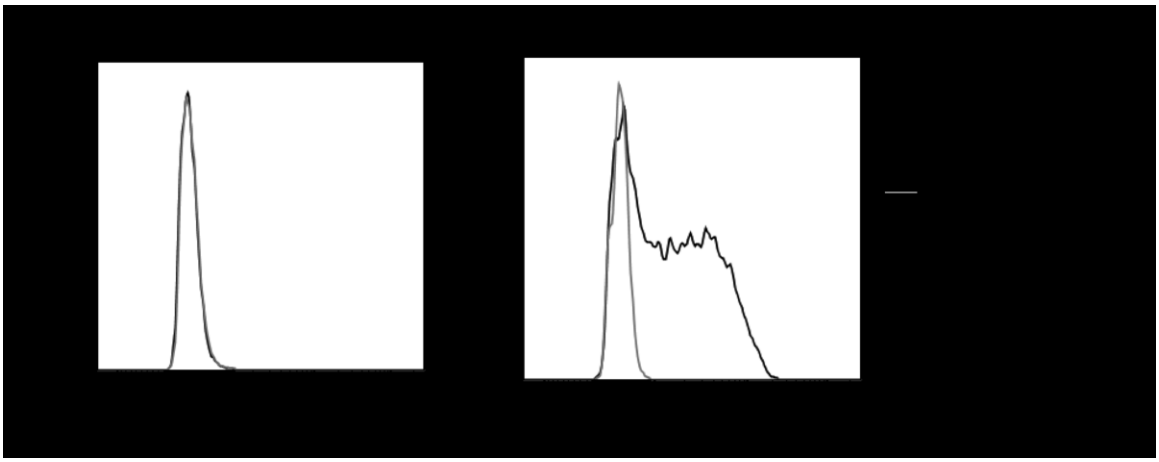

Figure 4.1. LILRA3-Fc binds to a ligand on K562 cells

Representative histogram data (n = 2) of binding assays of K562 with LILRA3-Fc at 1.1 μM.

4.2.2. K562 cells express a Nogo isoform extracellularly

The interaction of LILRA3 with K562 cells and the aforementioned finding that Nogo66 was a ligand of LILRA3 drove me to explore whether K562 cells expressed an isoform of Nogo on the surface. Nogo-B was reportedly ubiquitously expressed either intracellularly, extracellularly, or both [67]. I acquired an antibody raised against the C-terminus of Nogo, which is common to all Nogo isoforms. I tested the K562 and 221 cell lines for intracellular and extracellular expression of Nogo. The intracellular staining of both cell lines was characterised with high levels of background binding, not allowing me to ascertain whether there was any Nogo intracellular expression (Figure 4.2.A). However, the flow cytometry histogram plots pointed to extracellular expression of Nogo on the surface of K562 cells but not on the surface of 221 cells. I followed up the flow cytometry staining with a western blot after lysing 10 million cells per run for each cell line (Figure 4.2.B). The presence of bands across all 3 cell lines lane on the Western blot, suggest the potential for non-specific binding of the antibodies or the expression of different Nogo isoforms in all three cell lines. The black arrows indicate expected sizes of Nogo-B and Nogo-C on a reducing Western blot. According to the literature [73], Nogo-A runs at around 250 kD and wasn't visible on the Western blot.

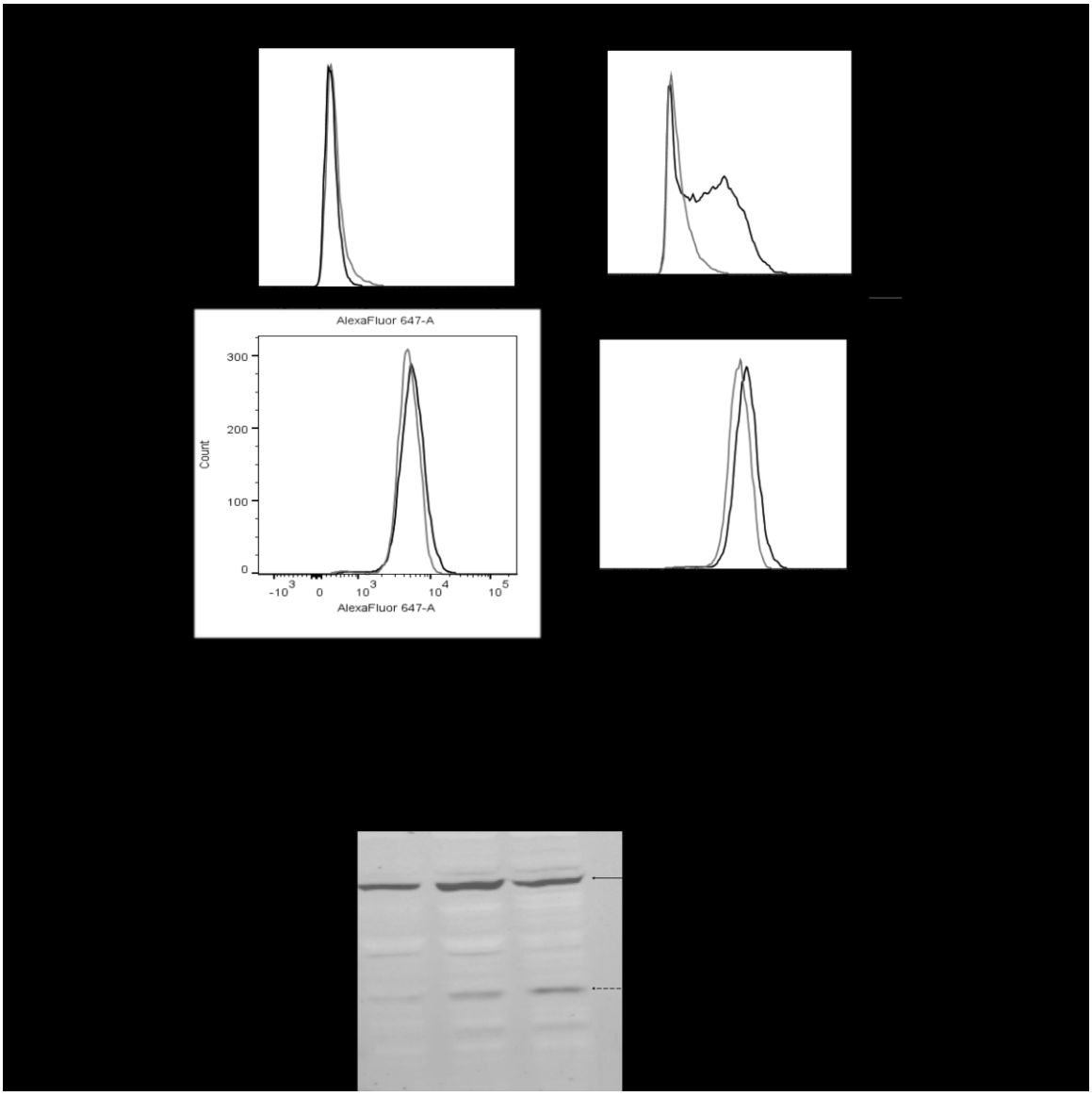

Figure 4.2. K562 cells express a Nogo isoform on their surface

A) Intracellular and extracellular staining of 221 and K562 cells with anti-Nogo antibody. B) Western blot of 221, 221-OMgp, and K562 cells and detection of Nogo isoforms with an anti-Nogo antibody, the black arrows indicate the expected sizes of Nogo-B (56 kDa) and Nogo-C (30 kDa).

The disconnect between the flow cytometry and Western blot results led me to perform a reverse-transcription PCR (RT-PCR). I designed primers that can specifically amplify and detect Nogo-A, Nogo-B, Nogo-C, and Actin expression from extracted total RNA from 221 and K562 cells (Figure 4.3). The RT-PCR results indicated that Nogo-C was expressed in K562 cells as well as 221 cells, whereas there was no detectable expression of Nogo-A and Nogo-B. This gel is a representation of three repeats with similar results obtained, with sections of the gel running unequally as it moved in the gel rig.

There is a further disconnect with the results of the Western blot and the RT-PCR. While Nogo-B appears in the Western blot for 221 and K562 cells, it does not in the RT-PCR. Nogo-C is the only Nogo isoform that appears in the RT-PCR, which appears for K562, 221, and 221-OMgp cells in the Western blot. It is possible that the Western blot band at 50 kDa is not Nogo-B. It is also possible that the RT-PCR did not pick up Nogo-B gene expression. We would need to validate the RT-PCR with a known Nogo-B expressing-line to determine whether we can pick up the gene's expression with the set of primers used. The only Nogo isoform that was picked up on the Western blot and the RT-PCR is Nogo-C. K562 cells and 221 cells express Nogo-C, but only K562 cells have detectable extracellular expression of Nogo through flow cytometry. Perhaps only K562 cells express Nogo-C on their surface. It is also possible that the signal picked up by flow cytometry may be a false positive and LILRA3 binds to another non-MHC ligand on K562. In fact, while Nogo and different HLA-I molecules have been identified as ligands of LILRA3, screens have

picked up the 67 kDa laminin receptor as a potential ligand for LILRA3 [55], but this has yet to be confirmed in binding assays.

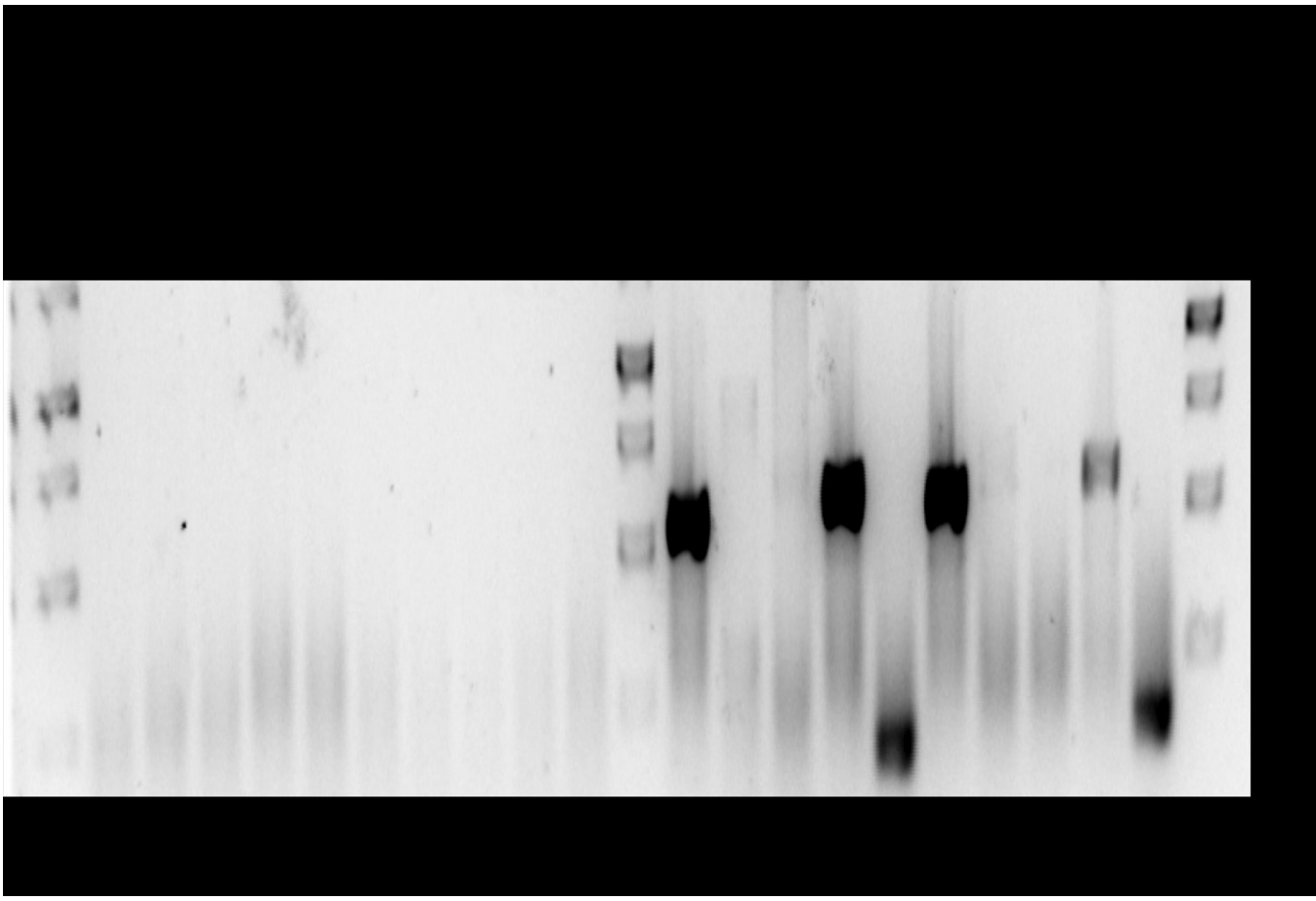

Figure 4.3. K562 and 221 cells have detectable Nogo-C message expression

RT-PCR gel of 221 and K562 cells with Nogo, Nogo-A, Nogo-B, Nogo-C, and Actin (loading control) specific primers.

4.2.3. Addition Nogo66 40-mer influences the binding of LILR-Fc to their ligands

Having established the potential expression of Nogo-C on the surface of K562, I wanted to determine whether adding the Nogo66 40-mer to a binding assay of LILRA3 to K562 would block the interaction. If there was indeed an impact of the binding of LILRA3 to K562 in the presence of the Nogo66 40-mer, would that impact be seen if the Nogo66 peptide was added to binding assays of LILRA3 and LILRB2 with 221-OMgp and 221-HLA-G? To test this hypothesis, I pre-incubated the LILRA3-Fc with the Nogo66 40-mer peptide at different molar equivalencies, then added the peptide and LILR-Fc complex to the K562 cells. At a 1:1 molar ratio between LILRA3-Fc and Nogo66 40-mer, there was an unexpected enhancement in total geometric mean fluorescence intensity to the K562 cells. The trend of increasing fluorescence intensity plateaus at the 5:1 and 10:1 molar ratios of Nogo66 (40-mer):LILRA3-Fc (Figure 4.5). The histogram profiles accompanying the increases in fluorescence show two distinct peaks forming with the increased addition of Nogo66 40-mer peptide (Figure 4.4). The first peak at a relatively low fluorescent levels (Low PE in Figure 4.5) with a large cell count keeps decreasing in fluorescence with the increased molar concentration of the Nogo66 40-mer peptide. The second peak on the other hand has a relatively higher fluorescence (High PE in Figure 4.5) but with a depressed cell count based on the histogram relative to the no peptide added binding profile. Aggregating the data from the histogram plots and fluorescence quantification, the addition of the peptide to LILRA3-Fc contributed to the potential formation of a complex between LILRA3, Nogo66, and an unknown ligand on K562

cells which led to the initial increase in fluorescence. Concurrently, the peptide when added at a 5:1 and 10:1 ratio to LILRA3 compared to the 1:1 peptide:LILR binding profile, had a partial blocking effect on LILRA3 to a larger subset of the cells, indicating that the peptide potentially blocked the interaction between LILRA3 and a ligand found on the surface of K562 cells that shares the same binding site of LILRA3 to the Nogo66 40-mer peptide. These findings led me to focus on binding assays between LILRA3 and LILRB2 and their known ligands in the presence of the Nogo66 peptide.

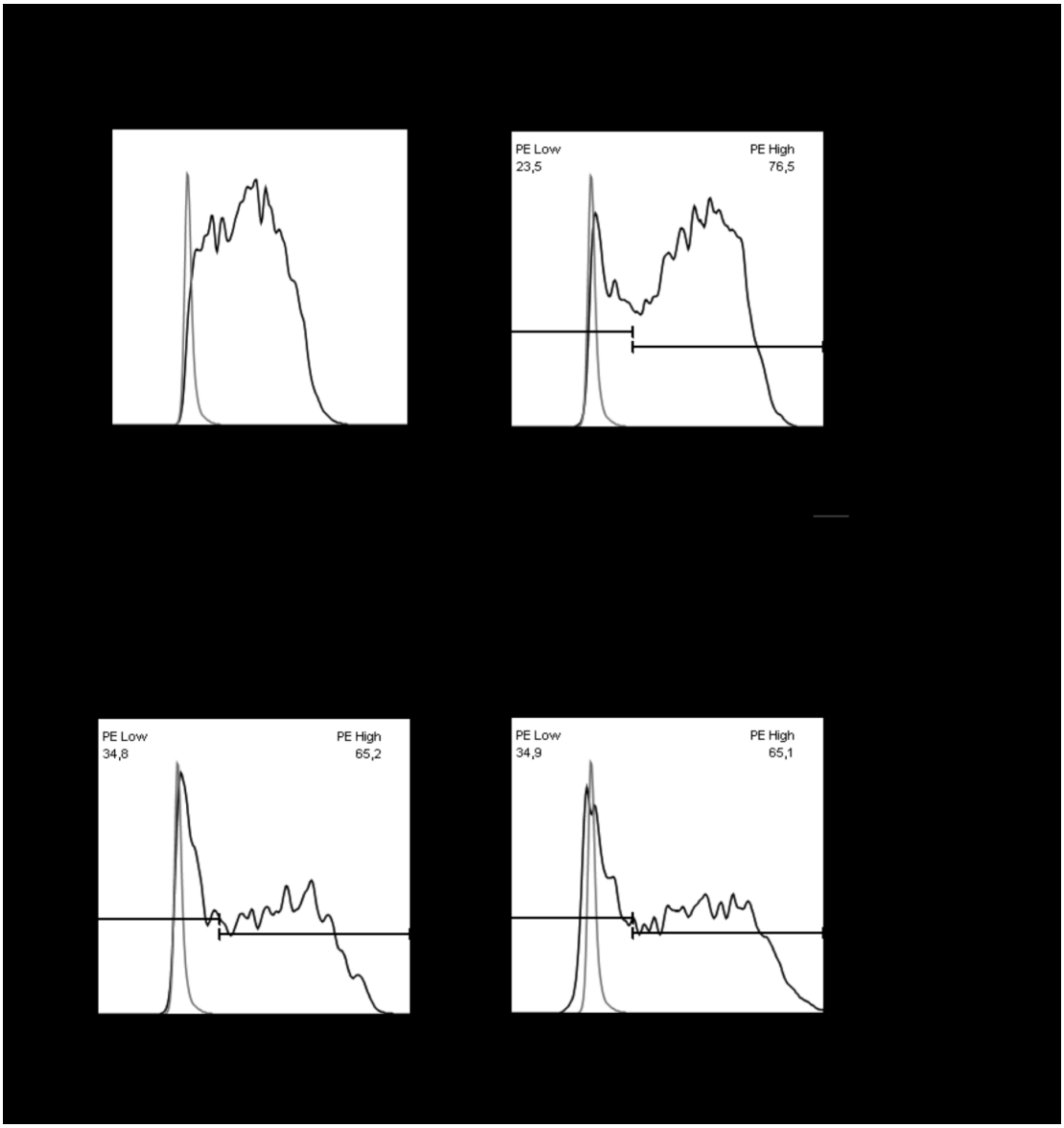

Figure 4.4. Addition of 40-mer Nogo66 peptide to LILRA3 enhances it's binding to K562 in a concentration dependent manner

Nogo66 40-mer was incubated with 1.1 μM LILRA3-Fc at different molar equivalencies for 1 hour then added onto K562 cells for another hour. Binding was detected by PE goat anti-Fc using flow cytometry.

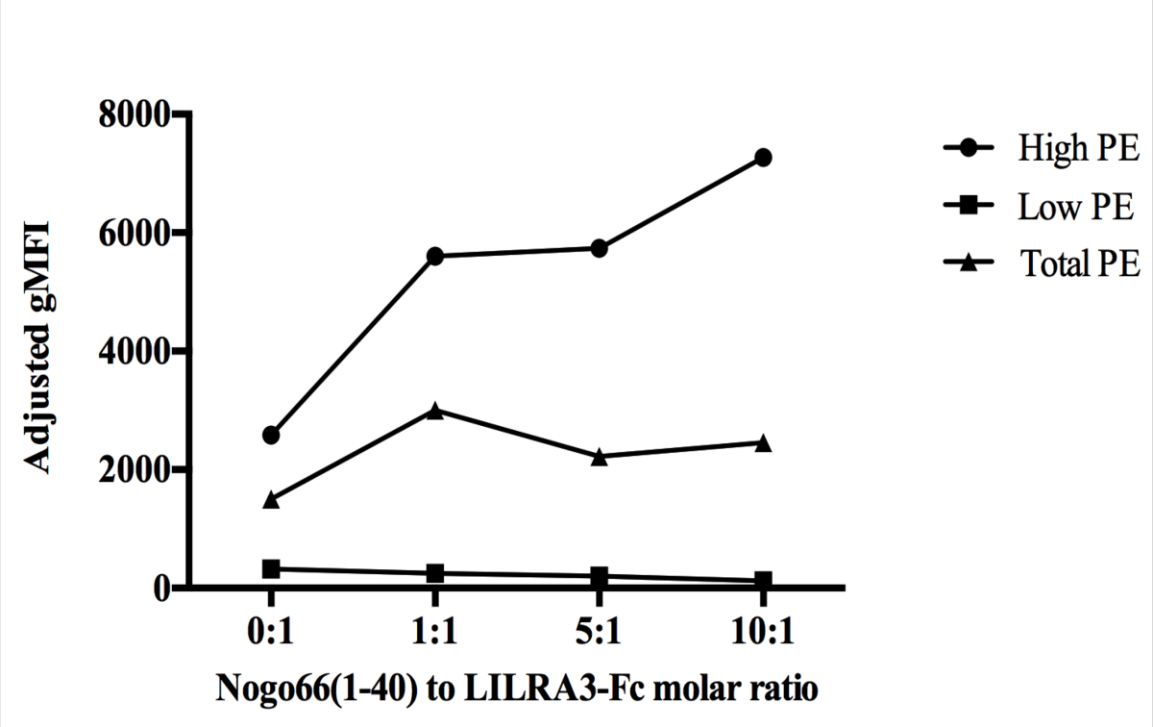

Figure 4.5. Quantifying the binding of LILRA3-Fc to K562 at 1.1 µM in geometric mean fluorescence intensity.

Binding of LILRA3-Fc quantified in adjusted gMFI (corrected for background), segregating between the highly fluorescent tails (High PE) and low fluorescence peak (Low PE) from figure 4.4 (n = 1).

After identifying the potential blocking capability of the Nogo66 40-mer peptide to the LILRA3-Fc-K562 interaction, I explored whether the peptide could block the LILRA3-OMgp interaction. I either added LILRA3-Fc to the 221 or 221-OMgp cells to determine binding, or added the pre-incubated complex of Nogo66 40-mer peptide and LILRA3-Fc at a 10:1 ratio to the 221 or 221-OMgp cells. Based on the histogram plots (Figure 4.6.A) and quantification of fluorescence (Figure 4.6.B), the presence of the Nogo66 40-mer peptide enhanced the interaction of LILRA3 and OMgp on a small subset of cells (High PE), as seen by the presence of a tail. There was no apparent blocking of the interaction as seen with the K562 cells, and the Nogo66 40-mer enhanced LILRA3-Fc binding to OMgp (Figure 4.7). The formation of the tail with the addition of the peptide to LILRA3-Fc could be due to the fact that I had not saturated the amount of LILRA3 binding to OMgp in the binding assay. I did not have the opportunity to saturate the amount of LILRA3-Fc binding to OMgp in the binding assays due to the limitations of obtaining large concentrations of purified LILRA3-Fc. These results suggest either one of the following, that Nogo66 peptide produces a conformation change in LILRA3-Fc that enhances the binding to OMgp, or that the Nogo66 peptide cross-links LILRA3-Fc while leaving the binding site between OMgp and LILRA3 unblocked.

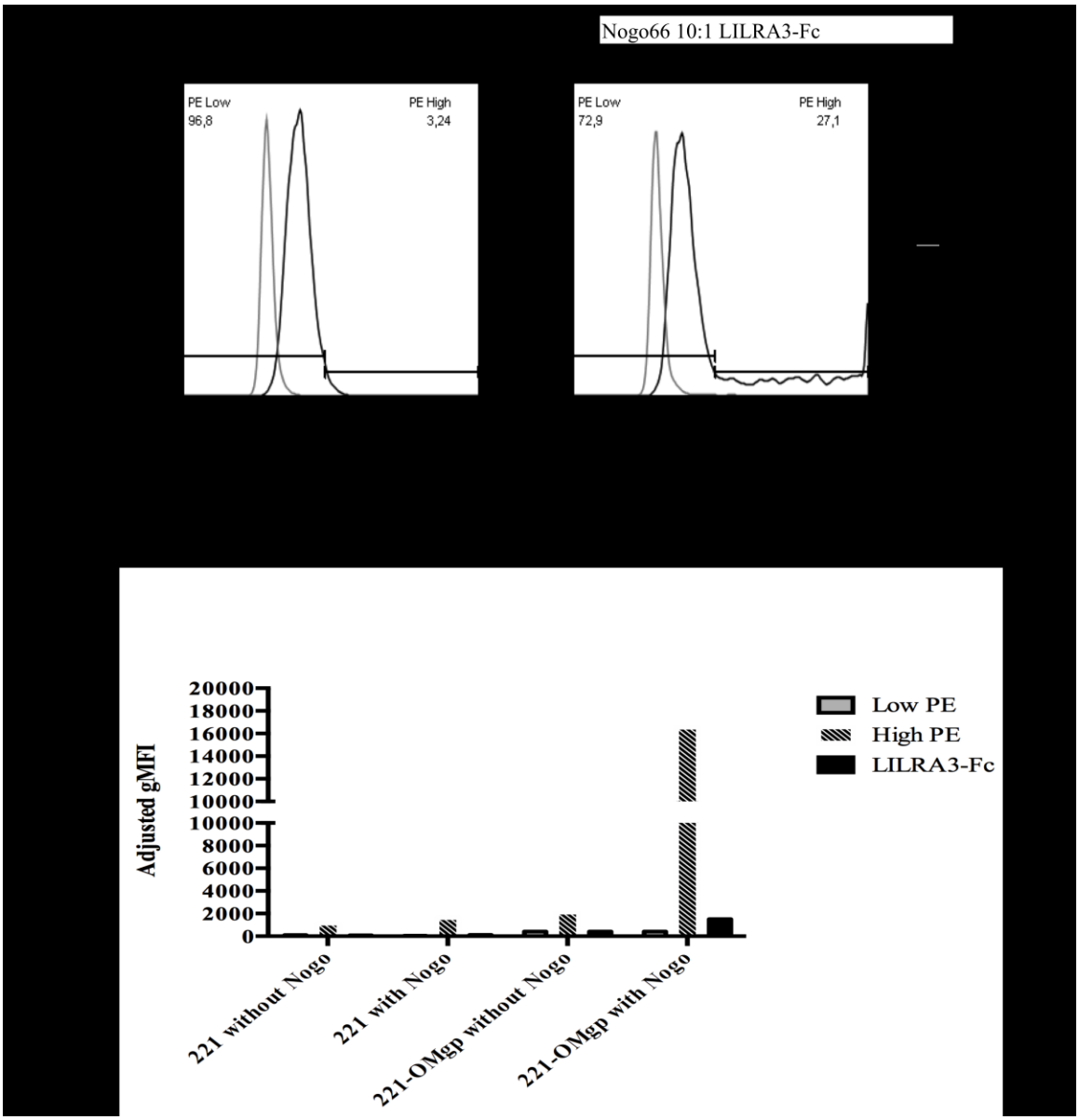

Figure 4.6. Nogo66(1-40) enhances LILRA3 binding to 221-OMgp

Nogo66 40-mer was incubated with 1.1 μM LILRA3-Fc at different molar equivalencies for 1 hour then added onto 221 and 221-OMgp cells for another hour. Binding was detected by PE goat anti-Fc using flow cytometry. A) Representative histogram; B) Binding quantified by gMFI after correcting for the background and segregated based on the fluorescence of the peak (Low PE) and the highly fluorescent tail (High PE). Representative data of n = 3.

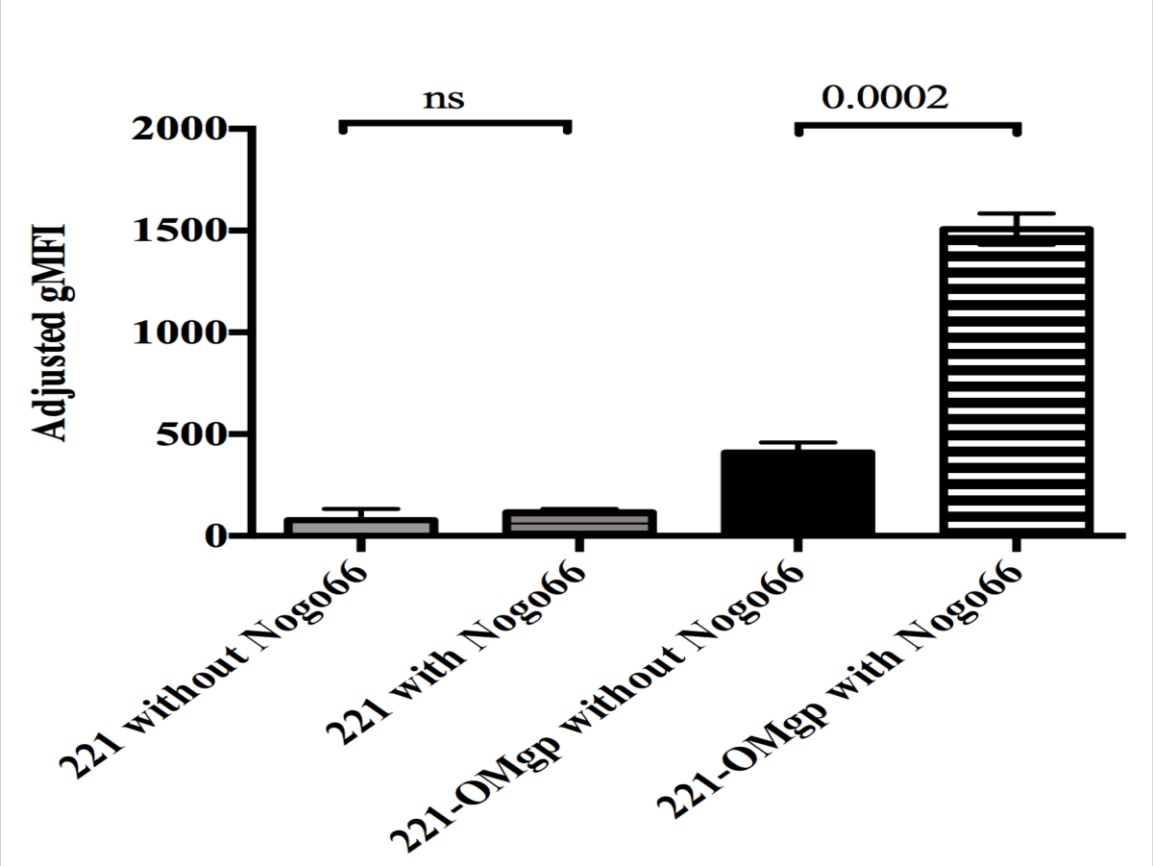

Figure 4.7. Aggregate data of LILRA3-Fc binding to 221-OMgp in the presence of Nogo66(1-40) peptide

The gMFI was quantified aggregated over three experiments after correcting for the background. An unpaired student t-test was performed for statistical analysis (n =3).

With the results from the previous experiments suggesting that the Nogo66 40-mer peptide enhanced the binding of LILRA3 to OMgp, I wanted to determine whether this enhancement was dose-dependent. I used the Nogo66 40-mer peptide at different molar equivalency ratios to LILRA3 and assessed the binding to 221-OMgp cells. With increasing molar concentrations of Nogo66, the LILRA3 binding to 221-OMgp was enhanced at 1:1, 5:1, and 10:1 ratios of Nogo66 40-mer:LILRA3-Fc (Figure 4.8). In addition, the increasing amounts of Nogo66 peptide had no effect on the binding of LILRA3 to 221 cells, indicating that the effect seen is specific to 221-OMgp and K562 cells. This enhancement seen on these two cell lines could simply be driven by the presence of LILRA3 ligand on the surface of these cells, which in the case of 221-OMgp cellsit most certainly is OMgp. As for K562, an RNAi screen could elucidate the LILRA3 ligand responsible for the binding of LILRA3-Fc and the Nogo-66-mediated binding enhancement. These results also confirmed that the Nogo66 peptide did not block the interaction between LILRA3 and OMgp. This, combined with the results from the previous experiments points to OMgp and Nogo66 not sharing the same contact sites on LILRA3.

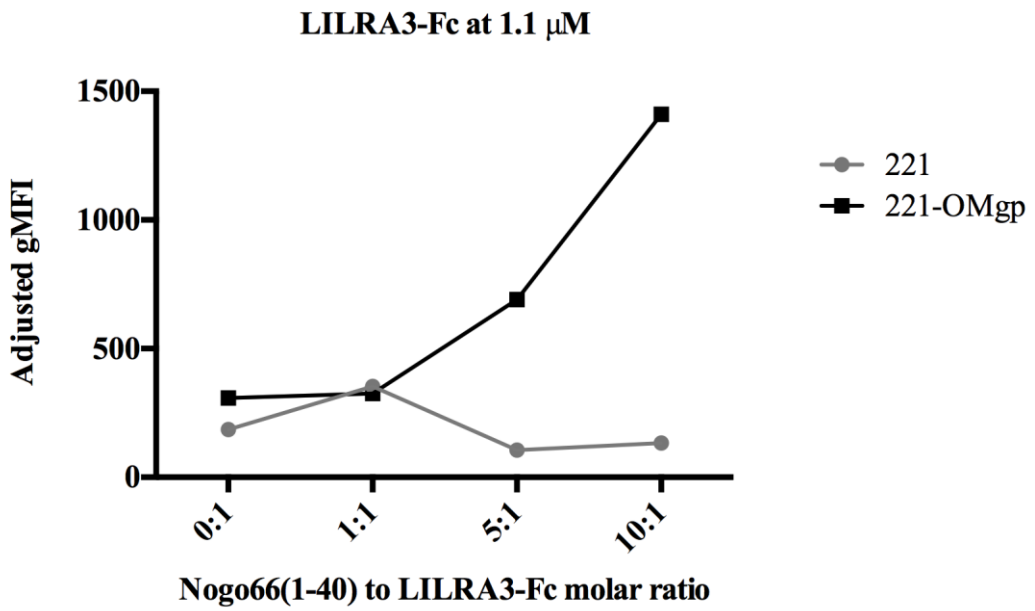

Figure 4.8. Nogo66(1-40) enhances LILRA3 binding to 221-OMgp in a concentration-dependent manner

Nogo66 40-mer was incubated with 1.1 μM LILRA3-Fc at different molar equivalencies for 1 hour then added onto 221 and 221-OMgp cells for another hour. Binding was detected by PE goat anti-Fc using flow cytometry and quantified gMFI after correcting for the background. Representative data (n = 2).

After establishing that the Nogo66 40-mer peptide enhanced the binding of LILRA3 to OMgp, I wanted to assess whether the Nogo66 40-mer peptide also enhanced the LILRB2 binding to OMgp and HLA-G.

I repeated the same experiments performed with LILRA3-Fc and the Nogo66 peptide with LILRB2-Fc. I pre-incubated the Nogo66 40-mer with LILRB2-Fc before adding them to the cells. In three independent experiments, the addition of the Nogo66 40-mer did not enhance the binding of LILRB2-Fc to OMgp, but enhanced its binding to HLA-G (Figure 4.9). This suggests different binding properties between LILRB2 and LILRA3 to OMgp and Nogo66. LILRB2 predominantly uses the D1D2 domains to bind to HLA-G, and the enhancement of binding mediated by Nogo66 could be driven by cross-linking LILRB2 or increasing the stability of the interaction through a conformational change.

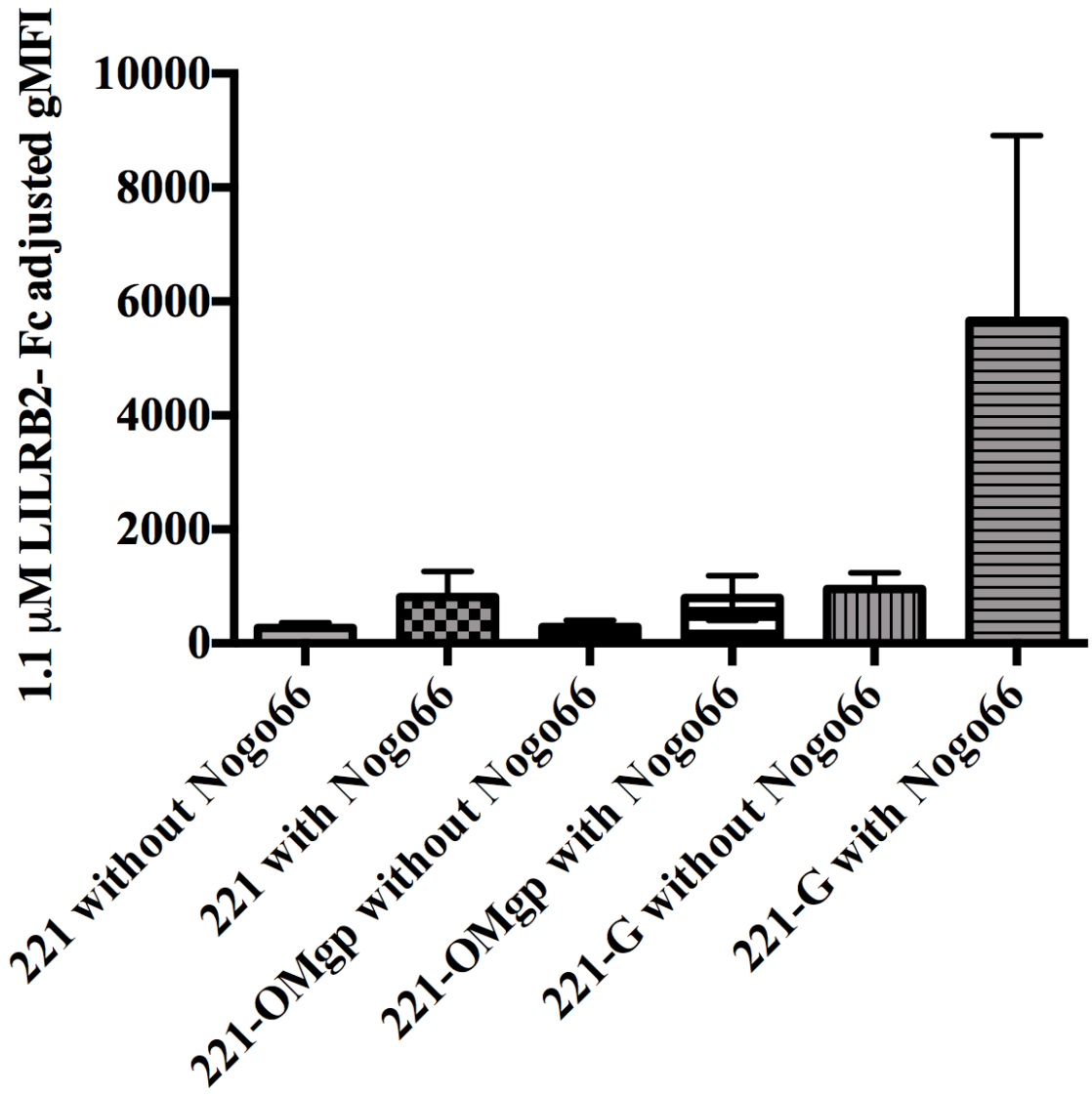

Figure 4.9. Nogo66(1-40) enhances LILRB2 binding to 221-HLA-G

Nogo66 40-mer was incubated with 1.1 μM LILRB2-Fc at different molar equivalencies for 1 hour then added onto 221, 221-OMgp, and 221-HLA-G cells for another hour. Binding was detected by PE goat anti-Fc using flow cytometry. Binding quantified by gMFI and aggregated over three experiments after correcting for the background and no statistically significant binding was observed. An unpaired student t-test was performed for statistical analysis (n = 3).

4.2.4. The Nogo66 40-mer mediated enhancement of LILRB2-Fc and LILRA3-Fc binding to HLA-G is blocked by an MHC-I-specific antibody

I wanted to verify the specificity of the enhanced binding observed in the presence of the Nogo66 40-mer. I designed the experiment by using the 221-G cells as HLA-G was a specific ligand of both LILRB2-Fc and LILRA3-Fc. I used an MHC-I antibody that blocked the interaction between LILRB2-Fc and HLA-G, as well as LILRA3-Fc and HLA-G. While pre-incubating LILRB2-Fc or LILRA3-Fc with the Nogo66 40-mer, I added the MHC-I blocking antibody to the cells. I transferred the antibody-cell complex to the tubes containing the LILRA3-Fc or LILRB2-Fc with the Nogo66 40-mer.

In the absence of the Nogo66 40-mer, the MHC-I blocking antibody blocked the interactions of LILRB2-Fc (Figure 4.10.A) and LILRA3-Fc (Figure 4.11.A) to the 221 cells expressing HLA-G. In the presence of the peptide, the same result occurs, with the LILRB2-Fc binding to HLA-G levels returning to the levels seen in the absence of the peptide. This result was confirmed when looking at the gMFI ratio of anti-MHC-I/Isotype in the presence and absence of the peptide was similar over three repeats. The binding of LILRA3-Fc to HLA-G in the presence of the Nogo66 40-mer was predictably enhanced. With the addition of the anti-MHC-I antibody, the LILRA3-Fc binding to HLA-G was partially blocked, with a high fluorescence tail showing on the histogram plot. This partial blocking of the LILRA3-Fc and HLA-G binding was also seen when no Nogo66 40-mer peptide was added. The reduced blocking manifested itself in the gMFI ratio of anti-MHC-I/Isotype over three repetitions being different when comparing gMFI with or without the Nogo66 40-

mer. This is probably due to the fact that the enhancement of LILRA3-Fc binding to HLA-G led to a significantly higher gMFI compared to the binding with no Nogo66 40-mer added.

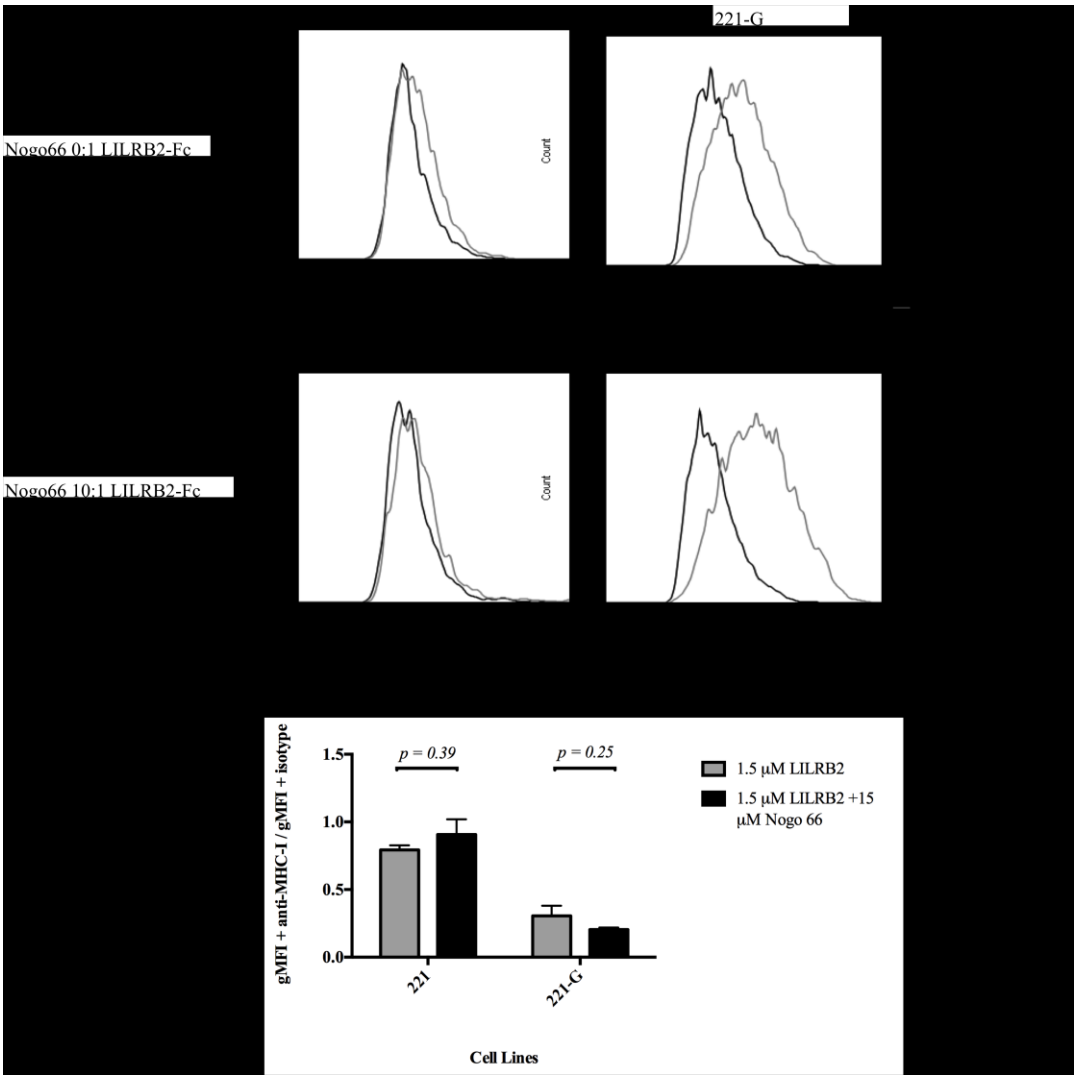

Figure 4.10. Nogo enhancement of LILRB2 binding to 221-G is blocked by anti-MHC-I antibody

1.5 µM LILRB2-Fc was incubated in the presence or absence of Nogo66 peptide for 1 hour then added onto 221 and 221-HLA-G pre-incubated with anti-MHC-I or isotype control. Binding was detected by PE goat anti-Fc using flow cytometry. A) Representative histogram data (n = 3). B) Ratio of adjusted gMFI (corrected for background) in the presence of anti-MHC-I against isotype control with or without the Nogo66 peptide, aggregated experiments (n = 3). An unpaired t-test was performed.

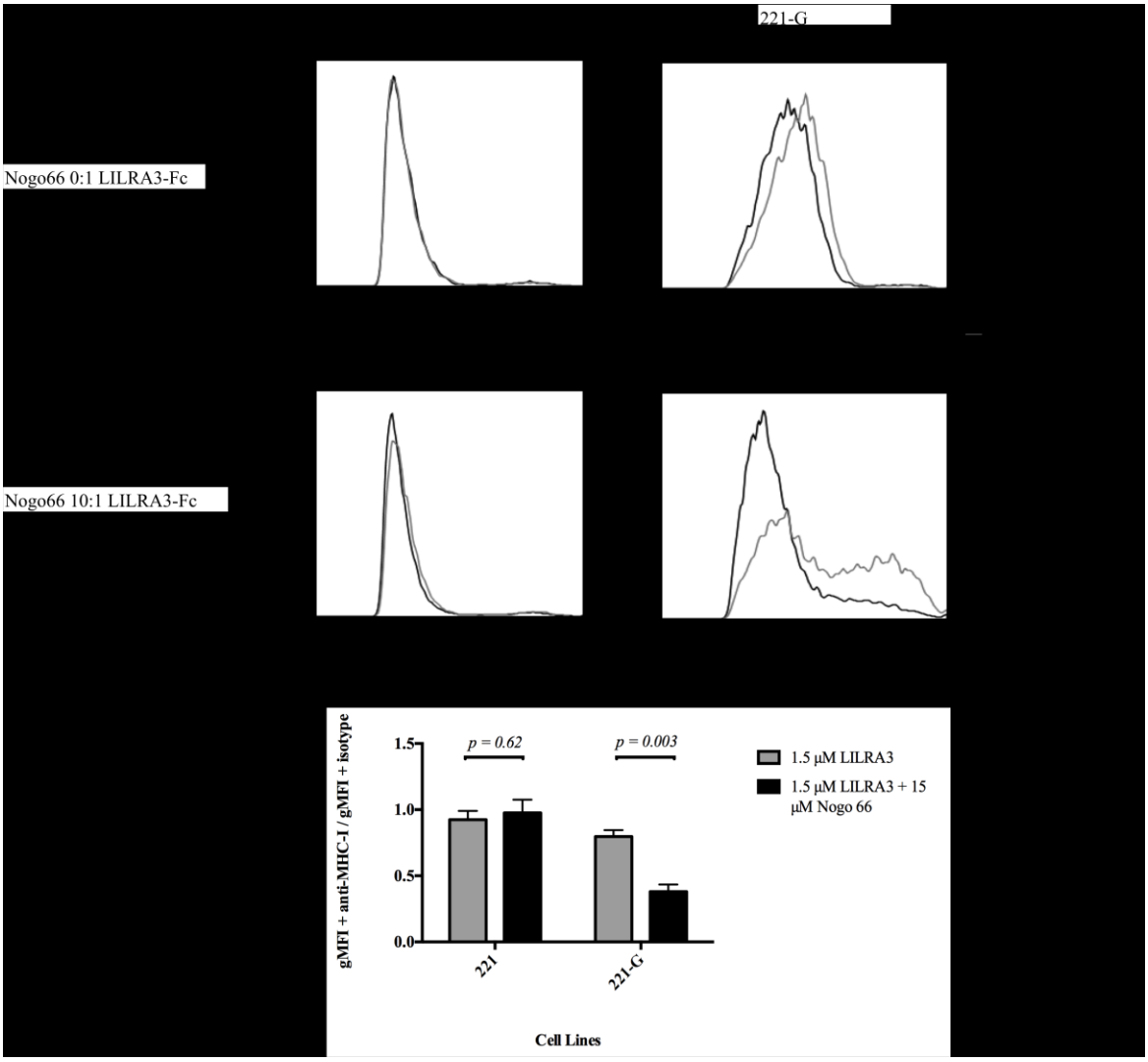

Figure 4.11. Nogo enhancement of LILRA3 binding to 221-G is blocked by anti-MHC-I antibody

1.5 µM LILRA3-Fc was incubated in the presence or absence of Nogo66 peptide for 1 hour then added onto 221 and 221-HLA-G pre-incubated with anti-MHC-I or isotype control. Binding was detected by PE goat anti-Fc using flow cytometry. A) Representative histogram data (n = 3). B) Ratio of adjusted gMFI (corrected for background) in the presence of anti-MHC-I against isotype control with or without the Nogo66 peptide, aggregated experiments (n = 3). An unpaired t-test was performed.

Chapter 5

Discussion

5.1. Summary of Results Section

Recent evidence in the literature identifying novel ligands for the Leukocyte Ig-Like Receptor family has generated new predictions regarding the role of these receptors in multiple contexts. The findings showing that LILRB2 and LILRA3 can bind to molecules found on the myelin sheath, coupled with their immunoregulatory functions, suggest a role for LILRB2 and LILRA3 in neuro-inflammatoin. In this thesis, I examined the interactions of LILRB2 and LILRA3 with two members of the myelin-associated inhibitors (MAI), OMgp and Nogo. In chapter 3, I was able to show that LILRB1 had no interaction whatsoever with OMgp in a direct ELISA, whereas LILRA3 and LILRB2 did. The trend from the ELISA results suggested that LILRA3 had a stronger interaction with OMgp than LILRB2. Using purified LILRA3-Fc and LILRB2-Fc, I was able to show that both fusion proteins can bind to 221 cells expressing OMgp on their surface. These experiments were done using flow cytometry-based binding assays and LILRA3 and LILRB2 exhibited similar binding strength to 221-OMgp cells. I was also able to show that LILRB2 and LILRA3 can bind to 221 cells expressing HLA-G using the same flow-cytometry based assay. LILRB2 showed stronger binding to HLA-G than LILRA3, and the binding specificity was determined using the blocking antibody W6/32. Furthermore, I was able to partially domain map the interaction of LILRA3 to HLA-G, after purifying the two membrane distal domains (D1D2-LILRA3-Fc) and two membrane proximal domains (D3D4-LILRA3-Fc). I could not obtain a sufficient yield of the purified D3D4-LILRA3-Fc due to stability to run the binding assays, but D1D2-LILRA3-Fc bound specifically to the 221-G cells.

In chapter 4, after the Nogo66 domain of Nogo was identified as a high affinity ligand for LILRA3 [55], I examined the binding properties of the LILRs to HLA-G and OMgp in the presence of a Nogo66 40-mer peptide. I found that the addition of a Nogo66 40-mer enhanced the binding of LILRB2 and LILRA3 to HLA-G. The binding was reversed when the MHC-I blocking W6/32 antibody was added suggesting that the enhanced binding was specific to MHC-I. I was also able to show that the addition of the Nogo66 40-mer enhanced the binding of LILRA3 to OMgp. On the other hand, the addition of Nogo66 did not enhance the binding of LILRB2 to OMgp. This indicated that the binding enhancement was specific to OMgp binding only with LILRA3.

These findings lead to questions about the properties of the interactions of the LILRs and the MAIs. In addition, a better understanding of how the LILR-MAI interactions relate to the interactions between the LILRs and MHC-I molecules is required. This would allow us to uncover the physiological role of the LILRs in contexts where multiple ligands are present. Here are the questions that would allow us to uncover the aforementioned properties and functions of the LILRs, which I will be discussing in the following sections:

- Can the binding of LILRA3 to OMgp be blocked through the addition of a blocking antibody or knocking down OMgp expression to determine LILRA3 specificity to OMgp on 221-OMgp?
- In a similar fashion to LILRB2, does LILRA3 bind to MAG, indicating that it binds to all members of the MAIs?

- What are the binding affinities of LILRA3 and LILRB2 to OMgp, and do they bind preferentially to different members of the MAIs?
- Which domains of LILRA3 and LILRB2 are involved in the binding to the myelin-associated inhibitors?
- If Nogo66 and HLA-G are co-expressed on the cell surface, will LILRB2 and LILRA3 exhibit an enhanced binding profile?
- If Nogo66 and OMgp are co-expressed on the cell surface, will LILRA3 exhibit an enhanced binding profile?
- Which domains of LILRB2 and LILRA3 are involved in the enhanced binding with HLA-G seen when the Nogo66 40-mer is added?
- LILRB2 interacting with HLA-G leads to SHP-1-mediated inhibitory signalling; would that response be altered if Nogo66 was co-expressed with HLA-G? Does LILRA3 block or attenuate this response?
- In addition to the inhibition of neurite outgrowth, does LILRB2 expressed on the surface of APCs interacting with the MAIs lead to an immunological function?

5.2. Future Directions

5.2.1 Interactions of LILRB2 and LILRA3 to the MAIs

The reported binding of LILRA3 to OMgp is the first report to my knowledge suggesting an interaction between both proteins. In addition, I confirmed the findings of Atwal *et al*. [3] by showing that LILRB2 could also bind to OMgp in our flow cytometry based binding assays. Based on the observations that MAIs share a

common receptor in NgR1 [62] and LILRB2 [34], I speculate that LILRA3 would also be able to bind to all 3 members of the MAI family. Furthermore and based on the evidence shown by Tedla's group [1], I predict that LILRA3 antagonizes LILRB2 binding to OMgp and MAG in addition to Nogo. Using a direct ELISA and a flow cytometry-based system I showed that LILRA3 and LILRB2 bind to OMgp. The motivation to test the binding in the flow cytometry-based assay was to mimic as close as possible physiologic conditions. This entailed having OMgp expressed on the surface of a cell line, with soluble LILRA3 added. Soluble LILRB2 was also used in this assay, which isn't physiologically relevant, as LILRB2 is exclusively expressed on cell surfaces. Investigating the binding of LILRB2 to OMgp could have been done using a signalling reporter assay. This entails having LILRB2 expressed on a cell surface binding to OMgp on a separate cell surface, which would lead to a detectable decrease in the cell's function. While there was one previous report showing that LILRB2 could bind to OMgp [3], I am the first to report the binding of LILRA3 to OMgp (Figure 3.6). The binding detected by flow cytometry was not strong as evident by the low mean fluorescence intensities captured. I attempted to confirm the specificity of the binding of LILRA3 to OMgp by adding a polyclonal anti-OMgp antibody to block the binding. The addition of the polyclonal anti-OMgp antibody in the binding assay of LILRA3 to OMgp did not reverse or block the binding. Another method to confirm the specificity of the binding of LILRA3 to OMgp would have been to transfect the 221-OMgp cells with a siRNA targeting OMgp. I would initially test for the decreased expression of OMgp by Western blotting and flow cytometry in the OMgp siRNA-transfected cell line and the scramble si-RNA-transfected cell line.

The next step would be to compare the binding strength of LILRA3 and LILRB2 to the siRNA-transfected 221-OMgp cells with the 221-OMgp cells and look for a decrease in binding, which would indicate specific binding.

The same process that was followed to determine the binding of LILRA3 to OMgp would be followed to investigate the binding of LILRA3 to MAG. I would start by transducing MAG into 221 cells, and selectively enrich the highest expressors of MAG by sorting through flow cytometry or a serial limiting dilution. Once the high MAG expressors have been identified, I would perform flow-cytometry based binding assays with LILRA3 and LILRB2 to determine binding. In conditions where the binding of the LILRs to the MAIs yield low mean fluorescence intensity in the flow cytometry-based binding assay, I would need to confirm the binding specificity. The binding specificity of LILRA3 and LILRB2 would be determined using siRNA or a blocking antibody in a similar fashion to the method proposed above for OMgp. Another method to confirm the specificity of LILRA3 binding to OMgp on the surface of 221-OMgp cells would entail using soluble OMgp and pre-incubate it with LILRA3 before adding it to the 221-OMgp cells. Finally, this same process should be repeated with the different Nogo isoforms, as they all should have the Nogo66 loop domain on the cell's surface [74], which was identified as the domain with which LILRB2 and LILRA3 make contact [34, 55]. The motivation to confirm the binding of LILRB2 to all three MAIs using our flow-cytometry based model, with cell surface expression of the MAIs on 221 cells is since only one report has demonstrated LILRB2 binding to the MAIs [34].

5.2.2 Binding affinities of LILRB2 and LILRA3 to HLA-G and the MAIs

The identification of novel ligands of LILRB2 and LILRA3 adds more ligands to the long list of ligands these molecules have. Determining which ligands LILRB2 and LILRA3 bind preferentially to would be crucial to identify the functions of both LILRs *in vivo* in the presence of multiple ligands. We have a good knowledge of the binding affinities of LILRB2 and LILRA3 to some of their ligands. This understanding was gained using several methods, chief of which is surface plasmon resonance (SPR). SPR allows you to measure the on and off rates of ligands to their receptors which yields a dissociation constant. Using relatively small quantities based data can be collected on the binding kinetics and affinities of receptor-ligand interactions. SPR requires adding the ligand at saturating concentrations and not washing. Receptors are immobilized on a chip and the ligand in solution is run through, leading sensors to detect small changes in refraction driven by binding dynamics [75]. The output measured from SPR is the dissociation constant (K_d), which is a measure of binding affinity and the lower the dissociation constant, the stronger the binding.

The binding affinity of LILRB2 to UL-18 and several MHC-I molecules were previously determined through SPR [6,7]. Reports have shown that LILRB2 binds to UL-18, the CMV MHC-I mimic with a K_d of 12-14 μM, which is 3-fold higher than the binding affinity of LILRB2 to HLA-G monomer of 4.3 μM [76]. Another report investigated the binding affinities of the 2 membrane distal domains of LILRB2 (D1D2-LILRB2) and LILRA3 (D1D2-LILRA3) to HLA-G [48]. D1D2-LILRB2 had a binding affinity of 5.62 μM and D1D2-LILRA3 had a binding affinity of 14.6 μM

to HLA-G. These results suggest first of all that D1D2-LILRB2 has a higher affinity for HLA-G than does D1D2-LILRA3. These results agree with the flow cytometry-based binding assays I performed with LILRB2 and LILRA3 binding to 221-G cells (Figure 3.5). A flow cytometry-based binding assay only allows us to determine the relative strength of binding provided the concentration of ligands used is in the linear part of the binding curve. In my assays, the binding strength of LILRB2 to HLA-G appeared higher compared to LILRA3 when observed on the histogram plot. The difference in the binding affinities seen between full length LILRB2 and D1D2-LILRB2 to HLA-G in the two different reports could be due to the experimental conditions or point to a potential influencing role of the D3D4 membrane proximal domains of LILRB2. Structural models suggesting that the D3D4 domains of LILRB2 clamp down on the α1 and α2 chains of MHC-I molecules support this hypothesis [29]. The limitation of these studies revolved around the purification methods of the LILRs. These groups purified LILRs from bacterial cells, which lack the ability to generate post-translational modifications seen in mammalian proteins. Changes glycosylation have a significant impact on the binding of the LILRs to their binding, but also their function [50, 51]. In fact, data comparing a polymorphism of LILRB1, which resulted in a difference in glycosylation had a direct impact on their interactions with some of their ligands. The variant with an additional N-glycosylation was shown by Yu *et al.* to bind HLA-B and HLA-C more strongly in a flow cytometry-based binding assay [10]. The presence of this additional glycosylated site however had no impact on LILRB1 binding to HLA-G. Therefore, one explanation why there are differences in dissociation constants between each

report could be attributed to differences in protein production methods. These findings prompt us to confirm with mammalian purified LILRB2 and LILRA3 the dissociation constants observed in previous reports investigating the binding of LILRB2 and LILRA3 to HLA-G using SPR. I would expect the binding affinities of LILRB2 and LILRA3 to HLA-G would follow a similar trend to those observed in the flow cytometry-based binding assays performed. The dissociation constant of LILRB2 binding to HLA-G would be lower than LILRA3's dissociation constant. Only two reports have looked at the affinity of the interactions between the LILRs and the MAIs. The first report published by Takai's group analyzed, using SPR, the binding affinity of PIR-B and PIR-A and their various domains to Nogo66 [39]. While PIR-B has been used in different studies as the mouse homolog to LILRB1 and LILRB2 [3], PIR-A has not been recognized as a homolog to a particular member of the LILR family. However, both PIR-B and PIR-A have 6 extracellular Ig domains, unlike the 4 commonly found in most LILRs. The dissociation constant of PIR-B binding to Nogo66 was 0.57 μM, which was lower than the K_d of PIR-B to HLA-G (2.4 μM) and H-2D^b (4.0 μM). This suggests that PIR-B has a higher affinity to the Nogo66 domain of the Nogo isoforms than to the human MHC-I and mouse MHC-I. PIR-A on the other hand had a dissociation constant of 6.9 μM, indicating that PIR-B has a slightly higher affinity to Nogo66 than PIR-A. In a recent study, Tedla's group identified Nogo66 as a ligand of LILRA3 and performed an SPR analysis to determine the dissociation constant of this interaction [55]. The data indicated that Nogo66 is the ligand with the highest binding affinity to LILRA3 with a K_d value of 0.311 nM. The authors did not perform an SPR analysis of the interaction between

LILRB2 and Nogo66, but they set up what could be interpreted as a competitive binding assay. The assay consisted of culturing primary human foetal cortical neurons on a matrix, which express LILRB2 and adding Nogo66 with or without the LILRA3. In the presence of Nogo66, neurite outgrowth was inhibited, as measured by neuron length compared to the sample to which no Nogo66 was added. In the presence of Nogo66 and LILRA3, the inhibition of neurite outgrowth was reversed, suggesting that LILRA3 blocked the interaction between Nogo66 and LILRB2. While we do not have a precise measure of the binding affinity of LILRB2, reversing the inhibition of neurite outgrowth only required 100 nM of LILRA3. To obtain a precise measure of competitive binding, repeating a similar experiment would be required by titrating LILRA3 into the assay. This would allow me to identify the concentrations at which LILRA3 antagonizes the binding of LILRB2 to Nogo66. An analysis using SPR would be required to determine LILRB2's dissociation constant to Nogo66 to accurately compare it's binding affinity to the ligand with LILRA3's. In conditions where LILRB2 is potentially expressed on axons in a similar fashion to PIR-B in mice, the Nogo66 domain of Nogo-A in myelin would be in contact with LILRB2, thereby inhibiting neurite outgrowth. If microglia or CNS invading monocytes were to secrete LILRA3, it would take a certain level of induction of LILRA3 expression to antagonize LILRB2 and block the inhibition of neurite outgrowth. This would lead to the regeneration of damaged axons. The binding of the LILRs to the MAIs can also come into play with released myelin fragments due to immune-mediated inflammation, in conditions such as multiple sclerosis. Antigen presenting cells expressing LILRB2 on their surface could bind to the MAIs on the damaged myelin

fragments, resulting in a potential inhibitory signaling cascade which would lead to non-clearance of myelin antigens. The secretion of LILRA3 would bind to the MAIs, outcompeting the LILRB2 binding, and coating the myelin antigens leading to their clearance and limiting their ability to further induce inflammation.

5.2.3 Nogo66-mediated binding enhancement of LILRB2 and LILRA3 to HLA-G and other ligands

After the identification of Nogo66 as a ligand for LILRB2 and LILRA3, I hypothesized that Nogo66 would block the interaction between the LILRs and MHC-I molecules. Surprisingly, I observed the opposite as binding assays of LILRA3 or LILRB2 to HLA-G in the presence of Nogo66 revealed unexpected partial enhancement in binding (Figure 4.9-11). This partial binding enhancement to HLA-G was reversed in the presence of a MHC-I blocking antibody, showing the increase in binding was specific for MHC-I. The binding profile seen on the flow cytometry-generated histograms was characterized by relatively high binding on few cells, and lower binding on the majority of cells. There are at least two potential mechanisms that could allow Nogo66 to enhance LILRs binding. Firstly, Nogo66 might effect a conformational change that increases the affinity for HLA-G (Figure 5.1.A). The second mechanism could be caused by the Nogo66 loop cross-linking the LILR molecules which leads to their aggregation (Figure 5.1.B). The latter would fit best with the binding profile seen on the histograms with a minority of cells binding high amounts of LILRA3.

In future, it would be interesting to determine which domains are required for the effect of Nogo66. We could perform domain mapping experiments, isolating individual or paired Ig domains of the LILRs to determine which ones are involved in the binding enhancement to their ligands in the presence of Nogo66. In addition to determining which Ig domains are involved in the Nogo66-mediated binding enhancement, domain mapping might allow us to understand why Nogo66 enhanced the binding of LILRA3 to OMgp but not LILRB2 to OMgp.

A complementary approach to domain mapping would be to co-crystallize the LILRs with members of the MAIs. This would allow us to precisely identify the contact sites and specific amino acids involved in the binding between the LILRs and the MAIs. The data obtained would be followed by mutating individual amino acids in the contact sites to confirm their effect on the binding of the LILRs to the MAIs. This set of data would complement the comprehensive set of mutational analyses performed on the LILRs and their interactions with MHC-I molecules [3]. The knowledge gained from knowing which amino acids are critical for the binding of the LILRs to the MAIs would allow us to understand their interactions with their diverse set of ligands in the different possible contexts and their function.

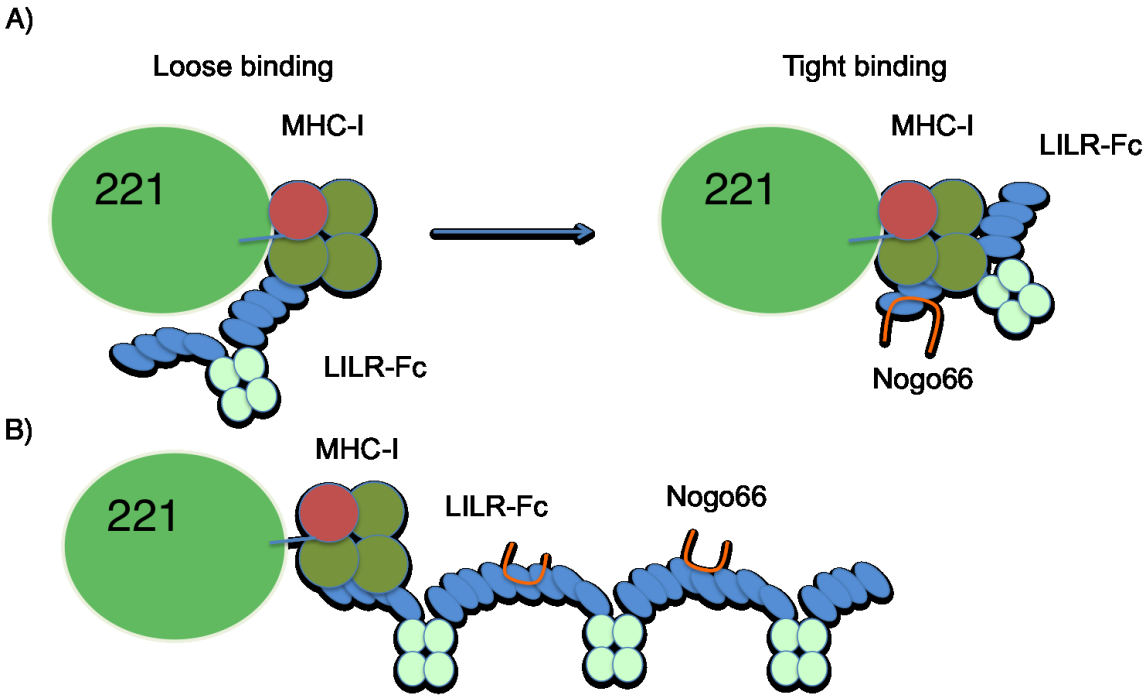

Figure 5.1. Models of LILR-Fc behaviour leading to the observed binding enhancement in the flow cytometry-based binding assays.

A) The presence of Nogo66 leads to a conformation change in the LILR-Fc, allowing it to bind the MHC-I ligand on the surface of the 221 cells more tightly. B) The presence of Nogo66 leads to the cross-linking of multiple LILR-Fc dimers leading to the aggregation of the LILR-Fc to the MHC-I ligand on the surface of 221 cells.

5.2.4 Interactions between LILRB2 and LILRA3 with the MAIs in the context of inflammation

The ability of LILRB2 and LILRA3 to bind to the Nogo66 domain present on all Nogo isoforms opens up the potential of these interactions to have functions in contexts outside of the known effects neurite outgrowth. Prior to their currently known function in the neurite outgrowth process, the LILRs were identified by their immunological functions. LILRB2 as an inhibitory receptor with ITIMs in its cytoplasmic tail has immunoregulatory functions on the surface of dendritic cells, while several reports suggested that LILRA3 as a soluble molecule has anti-inflammatory functions [3]. Based on the LILR-MAI axis of interaction, there are multiple contexts in which these receptor-ligand interactions can occur and lead to an immunological response. The first context would be in the case of CNS inflammation, whereby antigen-presenting cells expressing LILRB2 but also secreting LILRA3 would come into contact with myelin debris presenting MAIs on its surface [68]. The second context would involve Nogo-B expressed on the endothelium interacting APCs expressing LILRB2 on their surface or secreting LILRA3, which would potentially have consequences on the transmigration of these cells through the tissue based on several mouse models [66, 67]. Lastly, the final context to examine the LILR-MAI axis would be in immune-immune interactions. One report has shown gene expression of the MAIs in several immune cells [39] and understanding their role in that context and the potential of a functional interaction in cis or trans with LILRB2 on the surface of an APC and with LILRA3 would shed light on new functions of this axis of interaction.

Challenges would definitely arise in designing assays to test the interactions in these varying contexts and with human cells. Reductionist models would have to be developed, with APCs expressing LILRB2, LILRA3, and the MAIs naturally, siRNA knockdowns and knockouts targeting the individual molecules would be required. Furthermore, to develop an understanding of the function and signalling driven by these interactions, reporter systems would have to be designed. These reporter systems would involve cell lines of antigen presenting cells in which we can track phosphatase activities such as SHP-1 or SHP-2, which are recruited when LILRB2 is engaged. In addition, we would need to ensure that confounding variables such as MHC-I binding to LILRs are controlled for, especially in the case that Nogo66 expression may enhance the binding of the LILRs to them. The near ubiquitous expression of Nogo and MHC-I would pose a major challenge when it comes to attributing a certain response to LILRs interacting with either one of them. Introducing known blocking antibodies such as W6/32 (MHC-I blocking) would mitigate to a certain extent but not completely the risk of drawing conclusions from these experiments based on confounding variables.

5.3. Concluding remarks

The recent developments leading to the identification of new ligands of the LILRs, unrelated to the historically known classical and non-classical MHC-I molecules has led to more questions surrounding the functional nature of this receptor family. The implication of several members of the family in immune-mediate diseases and their interaction with ligands playing a role in these diseases requires an

understanding of the binding dynamics and resulting functions of these interactions. In the scope of my research, the interactions of LILRB2 and LILRA3 with members of the myelin-associated inhibitors led me to questions regarding the pathophysiology of multiple sclerosis. While the disease is characterized as a primarily immune-mediate disease, the role of LILRA3 and LILRB2 in neuron repair and damage respectively, could lead these molecules to be therapeutic targets in the near future. It is however crucial to understand the binding dynamics both LILRA3 and LILRB2 exert with both of their major ligand families, the MAIs and MHC-I molecules. The results discussed in this thesis first identified OMgp as a ligand of LILRA3, to complement the previous findings describing the interaction of LILRB2 to OMgp [34]. In the meantime, the conclusions from Tedla's group identifying the Nogo66 domain of Nogo as a ligand of LILRA3 [55], have allowed me to explore the binding dynamics of LILRA3 and LILRB2 to the non-classical MHC-I molecule HLA-G and OMgp in the presence of the now known ligand, Nogo66. The results have unexpectedly shown that LILRA3 can not only continue to interact with OMgp and HLA-G in the presence of Nogo66, but also show a pattern of enhanced binding. A similar pattern was observed with Nogo66 enhancing the binding of LILRB2 to HLA-G but not to OMgp, suggesting differences in the interactions between LILRA3 and LILRB2 with the MAIs. These interactions can also have consequences on other ligands the LILRs interact, notably LILRB2 which was shown to interact with many non-MHC-I ligands throughout different reports. Cementing and further understanding with precision these interactions will allow us to shed some light on

the function of these receptor-ligand interactions in the multiple possible contexts that were discussed.

Bibliography

1. Hirayasu, K. and H. Arase, *Functional and genetic diversity of leukocyte immunoglobulin-like receptor and implication for disease associations.* J Hum Genet, 2015.
2. Barrow, A.D. and J. Trowsdale, *The extended human leukocyte receptor complex: diverse ways of modulating immune responses.* Immunol Rev, 2008. **224**: p. 98-123.
3. Burshtyn, D.N. and C. Morcos, *The Expanding Spectrum of Ligands for Leukocyte Ig-like Receptors.* J Immunol, 2016. **196**(3): p. 947-55.
4. Samaridis, J. and M. Colonna, *Cloning of novel immunoglobulin superfamily receptors expressed on human myeloid and lymphoid cells: structural evidence for new stimulatory and inhibitory pathways.* Eur J Immunol, 1997. **27**(3): p. 660-5.
5. Wagtmann, N., et al., *A new human gene complex encoding the killer cell inhibitory receptors and related monocyte/macrophage receptors.* Curr Biol, 1997. **7**(8): p. 615-8.
6. Cosman, D., et al., *A novel immunoglobulin superfamily receptor for cellular and viral MHC class I molecules.* Immunity, 1997. **7**(2): p. 273-82.
7. Kubagawa, H., P.D. Burrows, and M.D. Cooper, *A novel pair of immunoglobulin-like receptors expressed by B cells and myeloid cells.* Proc Natl Acad Sci U S A, 1997. **94**(10): p. 5261-6.
8. Martin, A.M., et al., *Leukocyte Ig-like receptor complex (LRC) in mice and men.* Trends Immunol, 2002. **23**(2): p. 81-8.
9. Canavez, F., et al., *Comparison of Chimpanzee and Human Leukocyte Ig-Like Receptor Genes Reveals Framework and Rapidly Evolving Genes.* The Journal of Immunology, 2001. **167**(10): p. 5786-5794.
10. Zhang, G.J., et al., *Comparative Analysis of Bat Genomes Provides Insight into the Evolution of Flight and Immunity.* Science, 2013. **339**(6118): p. 456-460.
11. Hogan, L., et al., *Characterisation of bovine leukocyte Ig-like receptors.* PLoS One, 2012. **7**(4): p. e34291.
12. Campbell, K.S. and A.K. Purdy, *Structure/function of human killer cell immunoglobulin-like receptors: lessons from polymorphisms, evolution, crystal structures and mutations.* Immunology, 2011. **132**(3): p. 315-25.
13. Bashirova, A.A., et al., *Diversity of the human LILRB3/A6 locus encoding a myeloid inhibitory and activating receptor pair.* Immunogenetics, 2014. **66**(1): p. 1-8.
14. Borges, L., et al., *A family of human lymphoid and myeloid Ig-like receptors, some of which bind to MHC class I molecules.* Journal of Immunology, 1997. **159**(11): p. 5192-5196.
15. Fanger, N.A., et al., *The MHC class I binding proteins LIR-1 and LIR-2 inhibit Fc receptor-mediated signaling in monocytes.* Eur J Immunol, 1998. **28**(11): p. 3423-34.
16. Bellon, T., et al., *Mutational analysis of immunoreceptor tyrosine-based inhibition motifs of the Ig-like transcript 2 (CD85j) leukocyte receptor.* J Immunol, 2002. **168**(7): p. 3351-9.

17. Prod'homme, V., et al., *The human cytomegalovirus MHC class I homolog UL18 inhibits LIR-1+ but activates LIR-1- NK cells.* J Immunol, 2007. **178**(7): p. 4473-81.
18. Saverino, D., et al., *The CD85/LIR-1/ILT2 inhibitory receptor is expressed by all human T lymphocytes and down-regulates their functions.* Journal of Immunology, 2000. **165**(7): p. 3742-3755.
19. Chapman, T.L., A.P. Heikeman, and P.J. Bjorkman, *The inhibitory receptor LIR-1 uses a common binding interaction to recognize class I MHC molecules and the viral homolog UL18.* Immunity, 1999. **11**(5): p. 603-13.
20. Vitale, M., et al., *The leukocyte Ig-like receptor (LIR)-1 for the cytomegalovirus UL18 protein displays a broad specificity for different HLA class I alleles: analysis of LIR-1 + NK cell clones.* Int Immunol, 1999. **11**(1): p. 29-35.
21. Mamegano, K., et al., *Association of LILRA2 (ILT1, LIR7) splice site polymorphism with systemic lupus erythematosus and microscopic polyangiitis.* Genes Immun, 2008. **9**(3): p. 214-23.
22. Kuroki, K., et al., *Extensive polymorphisms of LILRB1 (ILT2, LIR1) and their association with HLA-DRB1 shared epitope negative rheumatoid arthritis.* Hum Mol Genet, 2005. **14**(16): p. 2469-80.
23. Chan, K.R., et al., *Leukocyte immunoglobulin-like receptor B1 is critical for antibody-dependent dengue.* Proc Natl Acad Sci USA, 2014. **111**(7): p. 2722-2727.
24. Nakayama, M., et al., *Inhibitory receptor paired Ig-like receptor B is exploited by Staphylococcus aureus for virulence.* J Immunol, 2012. **189**(12): p. 5903-11.
25. Arnold, V., et al., *S100A9 protein is a novel ligand for the CD85j receptor and its interaction is implicated in the control of HIV-1 replication by NK cells.* Retrovirology, 2013. **10**.
26. Riva, M., et al., *Induction of nuclear factor-kappaB responses by the S100A9 protein is Toll-like receptor-4-dependent.* Immunology, 2012. **137**(2): p. 172-82.
27. Shiroishi, M., et al., *Structural basis for recognition of the nonclassical MHC molecule HLA-G by the leukocyte Ig-like receptor B2 (LILRB2/LIR2/ILT4/CD85d).* Proc Natl Acad Sci U S A, 2006. **103**(44): p. 16412-7.
28. Chen, B., et al., *Role of HLA-B27 in the pathogenesis of ankylosing spondylitis (Review).* Mol Med Rep, 2017. **15**(4): p. 1943-1951.
29. Nam, G., et al., *Crystal structures of the two membrane-proximal Ig-like domains (D3D4) of LILRB1/B2: alternative models for their involvement in peptide-HLA binding.* Protein Cell, 2013. **4**(10): p. 761-70.
30. Chang, C.C., et al., *Tolerization of dendritic cells by T(S) cells: the crucial role of inhibitory receptors ILT3 and ILT4.* Nat Immunol, 2002. **3**(3): p. 237-43.
31. Vlad, G., et al., *Interleukin-10 induces the upregulation of the inhibitory receptor ILT4 in monocytes from HIV positive individuals.* Human Immunology, 2003. **64**(5): p. 483-489.

32. Beinhauer, B.G., et al., *Interleukin 10 regulates cell surface and soluble LIR-2 (CD85d) expression on dendritic cells resulting in T cell hyporesponsiveness in vitro.* Eur J Immunol, 2004. **34**(1): p. 74-80.
33. Xu, X., et al., *IL-10 enhances promoter activity of ILT4 gene and up-regulates its expression in THP-1 cells.* J Huazhong Univ Sci Technolog Med Sci, 2010. **30**(5): p. 594-8.
34. Atwal, J.K., et al., *PirB is a Functional Receptor for Myelin Inhibitors of Axonal Regeneration.* Science, 2008. **322**(5903): p. 967-970.
35. Li, D., et al., *A novel role of CD1c in regulating CD1d-mediated NKT cell recognition by competitive binding to Ig-like transcript 4.* Int Immunol, 2012. **24**(11): p. 729-37.
36. Zheng, J., et al., *Inhibitory receptors bind ANGPTLs and support blood stem cells and leukaemia development.* Nature, 2012. **485**(7400): p. 656-60.
37. Kim, T., et al., *Human LilrB2 is a beta-amyloid receptor and its murine homolog PirB regulates synaptic plasticity in an Alzheimer's model.* Science, 2013. **341**(6152): p. 1399-404.
38. Hofer, J., et al., *Ig-like transcript 4 as a cellular receptor for soluble complement fragment C4d.* FASEB J, 2016. **30**(4): p. 1492-503.
39. Matsushita, H., et al., *Differential but competitive binding of Nogo protein and class i major histocompatibility complex (MHCI) to the PIR-B ectodomain provides an inhibition of cells.* J Biol Chem, 2011. **286**(29): p. 25739-47.
40. Koch, S., et al., *Association of multiple sclerosis with ILT6 deficiency.* Genes Immun, 2005. **6**(5): p. 445-7.
41. Bonetti, A., et al., *A follow-up study of chromosome 19q13 in multiple sclerosis susceptibility.* J Neuroimmunol, 2009. **208**(1-2): p. 119-24.
42. Ordonez, D., et al., *Multiple sclerosis associates with LILRA3 deletion in Spanish patients.* Genes Immun, 2009. **10**(6): p. 579-85.
43. Wisniewski, A., et al., *6.7-kbp deletion in LILRA3 (ILT6) gene is associated with later onset of the multiple sclerosis in a Polish population.* Hum Immunol, 2013. **74**(3): p. 353-7.
44. Hirayasu, K., et al., *Evidence for natural selection on leukocyte immunoglobulin-like receptors for HLA class I in Northeast Asians.* Am J Hum Genet, 2008. **82**(5): p. 1075-83.
45. Hirayasu, K., et al., *Long-term persistence of both functional and non-functional alleles at the leukocyte immunoglobulin-like receptor A3 (LILRA3) locus suggests balancing selection.* Hum Genet, 2006. **119**(4): p. 436-43.
46. Ortiz, M.A., et al., *Influence of the LILRA3 Deletion on Multiple Sclerosis Risk: Original Data and Meta-Analysis.* PLoS One, 2015. **10**(8): p. e0134414.
47. An, H., et al., *Soluble LILRA3, a potential natural antiinflammatory protein, is increased in patients with rheumatoid arthritis and is tightly regulated by interleukin 10, tumor necrosis factor-alpha, and interferon-gamma.* J Rheumatol, 2010. **37**(8): p. 1596-606.

48. Ryu, M., et al., *LILRA3 binds both classical and non-classical HLA class I molecules but with reduced affinities compared to LILRB1/LILRB2: structural evidence.* PLoS One, 2011. **6**(4): p. e19245.
49. Jones, D.C., et al., *HLA class I allelic sequence and conformation regulate leukocyte Ig-like receptor binding.* J Immunol, 2011. **186**(5): p. 2990-7.
50. Lee, T.H., et al., *Glycosylation in a mammalian expression system is critical for the production of functionally active leukocyte immunoglobulin-like receptor A3 protein.* J Biol Chem, 2013. **288**(46): p. 32873-85.
51. Yu, K., et al., *LILRB1 polymorphisms influence posttransplant HCMV susceptibility and ligand interactions.* J Clin Invest, 2018.
52. Gonen-Gross, T., et al., *The CD85J/Leukocyte Inhibitory Receptor-1 Distinguishes between Conformed and 2-Microglobulin-Free HLA-G Molecules.* The Journal of Immunology, 2005. **175**(8): p. 4866-4874.
53. Giles, J., et al., *HLA-B27 homodimers and free H chains are stronger ligands for leukocyte Ig-like receptor B2 than classical HLA class I.* J Immunol, 2012. **188**(12): p. 6184-93.
54. Bowness, P., *Hla-b27.* Annu Rev Immunol, 2015. **33**: p. 29-48.
55. An, H., et al., *Soluble LILRA3 promotes neurite outgrowth and synapses formation through a high-affinity interaction with Nogo 66.* J Cell Sci, 2016. **129**(6): p. 1198-1209.
56. VanGuilder Starkey, H.D., et al., *Neuroglial expression of the MHCI pathway and PirB receptor is upregulated in the hippocampus with advanced aging.* J Mol Neurosci, 2012. **48**(1): p. 111-26.
57. Filbin, M.T., *Myelin-associated inhibitors of axonal regeneration in the adult mammalian CNS.* Nat Rev Neurosci, 2003. **4**(9): p. 703-13.
58. Prinjha, R., et al., *Inhibitor of neurite outgrowth in humans.* Nature, 2000. **403**(6768): p. 383-4.
59. Oertle, T. and M.E. Schwab, *Nogo and its paRTNers.* Trends in Cell Biology, 2003. **13**(4): p. 187-194.
60. Teng, F.Y. and B.L. Tang, *Cell autonomous function of Nogo and reticulons: The emerging story at the endoplasmic reticulum.* J Cell Physiol, 2008. **216**(2): p. 303-8.
61. Vourc'h, P. and C. Andres, *Oligodendrocyte myelin glycoprotein (OMgp): evolution, structure and function.* Brain Res Brain Res Rev, 2004. **45**(2): p. 115-24.
62. Fry, E.J., C. Ho, and S. David, *A role for Nogo receptor in macrophage clearance from injured peripheral nerve.* Neuron, 2007. **53**(5): p. 649-62.
63. Yu, J., et al., *Reticulon 4B (Nogo-B) is necessary for macrophage infiltration and tissue repair.* Proc Natl Acad Sci U S A, 2009. **106**(41): p. 17511-6.
64. Schanda, K., et al., *Nogo-B is associated with cytoskeletal structures in human monocyte-derived macrophages.* BMC Res Notes, 2011. **4**: p. 6.
65. Wright, P.L., et al., *Epithelial reticulon 4B (Nogo-B) is an endogenous regulator of Th2-driven lung inflammation.* J Exp Med, 2010. **207**(12): p. 2595-607.

66. Di Lorenzo, A., et al., *Endothelial reticulon-4B (Nogo-B) regulates ICAM-1-mediated leukocyte transmigration and acute inflammation.* Blood, 2011. **117**(7): p. 2284-95.
67. Kondo, Y., et al., *The Nogo-B-PirB axis controls macrophage-mediated vascular remodeling.* PLoS One, 2013. **8**(11): p. e81019.
68. Bar-Or, A., *The immunology of multiple sclerosis.* Semin Neurol, 2008. **28**(1): p. 29-45.
69. Vaughan, K., et al., *A molecular view of multiple sclerosis and experimental autoimmune encephalitis: what can we learn from the epitope data?* J Neuroimmunol, 2014. **267**(1-2): p. 73-85.
70. Karnezis, T., et al., *The neurite outgrowth inhibitor Nogo A is involved in autoimmune-mediated demyelination.* Nat Neurosci, 2004. **7**(7): p. 736-44.
71. An, H., et al., *Serum Leukocyte Immunoglobulin-Like Receptor A3 (LILRA3) Is Increased in Patients with Multiple Sclerosis and Is a Strong Independent Indicator of Disease Severity; 6.7kbp LILRA3 Gene Deletion Is Not Associated with Diseases Susceptibility.* PLoS One, 2016. **11**(2): p. e0149200.
72. Klein, E., et al., *Properties of the K562 cell line, derived from a patient with chronic myeloid leukemia.* Int J Cancer, 1976. **18**(4): p. 421-31.
73. Dodd, D.A., et al., *Nogo-A, -B, and -C are found on the cell surface and interact together in many different cell types.* J Biol Chem, 2005. **280**(13): p. 12494-502.
74. Schwab, M.E., *Functions of Nogo proteins and their receptors in the nervous system.* Nat Rev Neurosci, 2010. **11**(12): p. 799-811.
75. Patching, S.G., *Surface plasmon resonance spectroscopy for characterisation of membrane protein-ligand interactions and its potential for drug discovery.* Biochim Biophys Acta, 2014. **1838**(1 Pt A): p. 43-55.
76. Shiroishi, M., et al., *Efficient leukocyte Ig-like receptor signaling and crystal structure of disulfide-linked HLA-G dimer.* J Biol Chem, 2006. **281**(15): p. 10439-47.